Dalton Transactions

RSC Publishing

PAPER

View Article Online
View Journal

Cite this: DOI: 10.1039/c3dt51046h

New bisphosphomide ligands, 1,3-phenylenebis-((diphenylphosphino)methanone) and (2-bromo-1,3-phenylene)bis((diphenylphosphino)methanone): synthesis, coordination behavior, DFT calculations and catalytic studies†

Pawan Kumar,[a] Mujahuddin M. Siddiqui,[a] Yerrnaidu Reddi,[a] Joel T. Mague,[b] Raghavan B. Sunoj*[a] and Maravanji S. Balakrishna*[a]

The bisphosphomide, 1,3-{$Ph_2PC(O)$}$_2C_6H_4$ (**1**), was prepared by the reaction of isophthaloyl chloride with diphenylphosphine in the presence of triethylamine. The corresponding bromo-derivative, 2-Br-1,3-{$Ph_2PC(O)$}$_2C_6H_3$ (**2**), was obtained by the reaction of 2-bromoisophthaloyl chloride with diphenylphosphine. The reaction of **1** with elemental sulfur or selenium yielded the bis(chalcogenides), 1,3-{$Ph_2P(S)$-$C(O)$}$_2C_6H_4$ (**3**) and {1,3-$Ph_2P(Se)C(O)$}$_2C_6H_4$ (**4**). The reaction between **1** and [Ru(η^6-*p*-cymene)Cl_2]$_2$ and [Pd(η^3-C_3H_5)Cl]$_2$ in 1 : 1 stoichiometry yielded the corresponding binuclear complexes, [Ru_2(η^6-*p*-cymene)$_2Cl_4${1,3-{$Ph_2PC(O)$}$_2$(C_6H_4)}] (**5**) and [Pd_2(η^3-C_3H_5)$_2Cl_2${1,3-{$Ph_2PC(O)$}$_2$(C_6H_4)}] (**6**). The reaction of **1** with $AgClO_4$ followed by the addition of [Pd(COD)Cl_2] at room temperature resulted in the formation of a pincer complex [PdCl{2,6-{$Ph_2PC(O)$}$_2$(C_6H_3)}] (**9**), *via* transmetallation. Pincer complex formation through C–H activation requires drastic conditions and yields are generally moderate. The oxidative addition reaction between **2** and [Ni(COD)$_2$] gave a pincer complex [NiBr{2,6-{$Ph_2PC(O)$}$_2$(C_6H_3)}] (**8**), whereas the 2 : 1 reaction of **2** with [Pd_2(dba)$_3$] yielded the palladium analogue [PdBr{2,6-{$Ph_2PC(O)$}$_2$-(C_6H_3)}] (**9**) in quantitative yield. The reaction between **1** and CuX in a 1 : 1 molar ratio produced binuclear complexes, [Cu_2(μ-X)$_2${1,3-{$Ph_2PC(O)$}$_2$(C_6H_4)}$_2$] (**10**, X = Cl; **11**, X = Br; **12**, X = I), whereas the reaction between **1** and [Cu($NCCH_3$)$_4$]BF_4 led to the isolation of a spirocyclic complex, [Cu(CH_3CN)$_2${1,3-{$Ph_2PC(O)$}$_2$(C_6H_4)}]BF_4 (**13**). The silver complexes [Ag_2(μ-ClO_4)$_2${1,3-{$Ph_2PC(O)$}$_2$(C_6H_4)}$_2$] (**14**), [Ag_2(μ-OTf)$_2${1,3-{$Ph_2PC(O)$}$_2$(C_6H_4)}$_2$] (**15**) and [Ag_2X_2{1,3-{$Ph_2PC(O)$}$_2$(C_6H_4)}] (**16**, X = ClO_4; **17**, X = OTf) were obtained by treating **1** with $AgClO_4$ or AgOTf in 1 : 1 or 1 : 2 molar ratios. The reactions of **1** with [AuCl-(SMe_2)] in 1 : 1 and 1 : 2 molar ratios afforded mono- and binuclear complexes, [AuCl{1,3-{$Ph_2PC(O)$}$_2$-(C_6H_4)}$_2$] (**18**) and [Au_2Cl_2{1,3-{$Ph_2PC(O)$}$_2$(C_6H_4)}AuCl] (**19**), in good yield. The structures of complexes **5**, **7–10**, **12** and **14a** were confirmed by single-crystal X-ray diffraction studies. DFT calculations were performed in order to gain additional insights into the structure and bonding of the pincer complexes. An additional analysis of the orbital interactions in the case of palladium complex **9** is also included. The *in situ* generated rhodium complex of bisphosphomide **1** showed moderate to good selectivity in the hydroformylation of hex-1-ene and styrene derivatives.

Received 22nd April 2013,
Accepted 4th June 2013

DOI: 10.1039/c3dt51046h

www.rsc.org/dalton

Introduction

The recent interest in the chemistry of pincer ligands is primarily due to their rigid chelating ability which provides exceptional thermal stability[1] to the metal complexes. In addition, phosphorus based pincer ligands confer excellent electronic and steric tuning options around the metal center which makes them ideal candidates not only for homogeneous

[a]*Phosphorus Laboratory, Department of Chemistry, Indian Institute of Technology Bombay, Powai, Mumbai 400 076, India.*
E-mail: krishna@chem.iitb.ac.in, msb_krishna@iitb.ac.in, sunoj@chem.iitb.ac.in
[b]*Department of Chemistry, Tulane University, New Orleans, Louisiana 70118, USA*

†Electronic supplementary information (ESI) available. CCDC 934905–934911. For ESI and crystallographic data in CIF or other electronic format see DOI: 10.1039/c3dt51046h

catalysis but also in material applications.[2] The phosphorus based pincer ligands known in the literature are mainly of three types: PCP[3], PNP[4] and POP[5] with each one having either $-CH_2-$, –O– or –N′– (N′ = N(R) or NH) links or any of the two combinations[6] with phosphorus having alkyl, aryl, alkoxy, aryloxy or amino substituents. Pincer complexes are known to promote a variety of organic transformations, such as Aldol and Michael addition reactions,[7] C–C[8] and C–X (X = halogen) bond formation,[9] oxidative addition of C–O and C–F bonds,[10] polymerization of olefins,[11] alkane metathesis,[12] alkane dehydrogenation[13] as well as CO_2 [14] and N_2 [15] activation. Further, pincer complexes with PCCCP, PCNCP and PN(H)CN(H)P frameworks can also come across interesting reaction sequences involving reversible dearomatization which makes them an even more versatile catalytic system in organic synthesis,[16] in particular the direct synthesis of amides from alcohols and amines.[17]

Surprisingly, monophosphine or bis(phosphine) ligands based on carbonyl links also called phosphomides are less extensive and their coordination chemistry is scant. This may be due to the extreme sensitivity of P–CO bonds towards moisture.[18] A few known monophosphomide ligands along with compound IV, the only known bis(phosphomide), are given in Chart 1.[19]

The molybdenum,[19e] rhodium[19g] and iron[19f] complexes of ligands of the type I, III and IV are the only reported transition metal complexes with single crystal X-ray structure available only in the case of the rhodium complex [Cp*Rh($Ph_2PC(O)CH_3$)Cl_2].[19g] In view of this we sought to design pincer capable bis(phosphomide) ligands and wanted to explore their catalytic applications, in particular hydroformylation reactions, as to the best of our knowledge, the utility of pincer complexes in hydroformylation reactions is not known. As a continuation of our interest in designing new inexpensive ligands[20] and studying their transition metal chemistry and catalytic applications, we report on two new bis(phosphomide) ligands and their transition metal chemistry. The DFT calculations and the utility of rhodium(I) complex in hydroformylation reactions are also described.

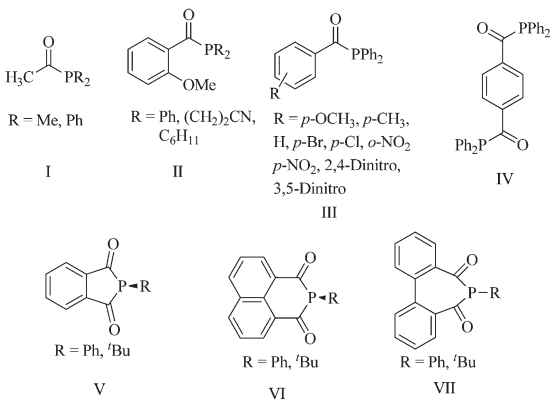

Chart 1

Results and discussion

Synthesis of 1,3-{$Ph_2PC(O)$}$_2$(C_6H_4) (1), 1-Br-2,6-{$Ph_2PC(O)$}$_2C_6H_3$ (2) and chalcogen derivatives

Nucleophilic substitution at carbonyl groups is the only feasible method for the synthesis of phosphomides where the choice of nucleophile mostly decides the rate as well as the reaction economy.[19] The bis(phosphomide), 1,3-{$Ph_2PC(O)$}$_2$-C_6H_4 (**1**), was synthesized in quantitative yield by the reaction of isophthaloyl chloride with diphenylphosphine in the presence of triethylamine (Scheme 1). Bis(phosphomide) **1** is a moisture sensitive and low melting yellow-orange solid soluble in most of the organic solvents. The $^{31}P\{^1H\}$ NMR spectrum of **1** consists of a single resonance at 12.3 ppm. The IR spectrum of **1** shows ν_{CO} at 1649 cm^{-1}.

The oxidation of bromo-*m*-xylene with $KMnO_4$ gave 2-bromoisophthalic acid, which on further treatment with $SOCl_2$ resulted in the formation of 2-bromoisophthaloyl chloride in moderate yield.[21] The 2-bromoisophthaloyl chloride was reacted with diphenylphosphine in the presence of triethylamine to obtain the bromo-functionalized bis(phosphomide), 1-Br-2,6-{$Ph_2PC(O)$}$_2C_6H_3$ (**2**), as a yellow solid in quantitative yield (Scheme 2). The $^{31}P\{^1H\}$ NMR spectrum of **2** shows a single resonance at 21.1 ppm.

The reaction of **1** with elemental sulfur or selenium in a 1 : 2 molar ratio in diethyl ether afforded the corresponding bis(chalcogenide) derivatives, 1,3-{$Ph_2P(S)C(O)$}$_2C_6H_4$ (**3**) and 1,3-{$Ph_2P(Se)C(O)$}$_2C_6H_4$ (**4**). The $^{31}P\{^1H\}$ NMR spectrum of **3** shows a single resonance at 38.1 ppm, whereas the selenide derivative **4** shows a major singlet at 31.1 ppm with characteristic selenium satellites. The $^1J_{PSe}$ coupling of 746 Hz is comparable with the same reported for analogous compounds in the literature.[22] Usually the magnitude of $^1J_{PSe}$ increases with an increase in electron withdrawing ability of the phosphorus substituents and *vice versa*. The electron withdrawing groups leave slightly less '*p*' and more '*s*' character in the lone pair which is eventually utilized in making P=Se bonds, as is

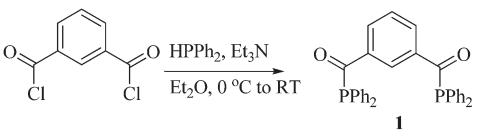

Scheme 1

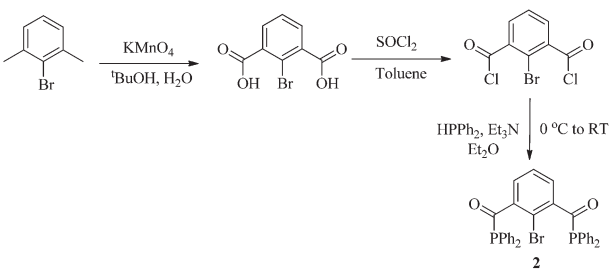

Scheme 2

reflected in the magnitude of the phosphorus–selenium coupling constant.

Synthesis of Ru and Pd complexes

The reaction of bis(phosphomide) **1** with one equiv. of $[Ru(\eta^6\text{-}p\text{-cymene})Cl_2]_2$ in dichloromethane afforded a binuclear complex, $[Ru_2(\eta^6\text{-}p\text{-cymene})_2Cl_4\{1,3\text{-}\{Ph_2PC(O)\}_2(C_6H_4)\}]$ (**5**). The 1 : 1 reaction between **1** and $[Pd(\eta^3\text{-}C_3H_5)Cl]_2$ resulted in the formation of a binuclear complex, $[Pd_2(\eta^3\text{-}C_3H_5)_2Cl_2\{1,3\text{-}\{Ph_2PC(O)\}_2(C_6H_4)\}]$ (**6**), in 89% yield (Scheme 3). The $^{31}P\{^1H\}$ NMR spectra of **5** and **6** consist of single resonances at 30.7 and 28.7 ppm, respectively.

Synthesis of Ni and Pd pincer complexes

Attempts to synthesize pincer complexes of platinum metals containing bis(phosphomide) (**1**) through C–H activation using well established methods even under drastic conditions have been unsuccessful. The coordination preferences of a pincer ligand is decisive in the formation of a pincer complex *via* C–H activation.[23] For pincer complex formation, the ligand has to optimize itself for suitable positioning of the donor arms. In addition, the reaction is believed to be electrophilic in nature and thus the higher electron density in the ring favors C–H activation.[24] In the case of PCP, POCOP and PNCNP types of pincer ligands the aromatic ring is electron rich because of the positive hyperconjugative or mesomeric effect of substituents which facilitates the C–H bond activation. In the case of bisphosphomide **1** the electron withdrawing carbonyl groups decrease the electron density at the *ipso* position which probably deters it to undergo C–H activation. However, the reaction of **1** with $AgClO_4$ followed by transmetallation with $[Pd(COD)Cl_2]$ in dichloromethane at room temperature yielded the desired pincer complex $[PdCl\{2,6\text{-}\{Ph_2PC(O)\}_2(C_6H_3)\}]$ (**7**) in moderate yield as shown in Scheme 4. The $^{31}P\{^1H\}$ NMR spectrum of complex **7** consists of a single resonance at 49.3 ppm.

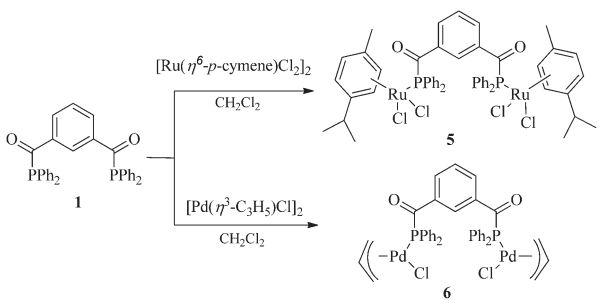

Scheme 3

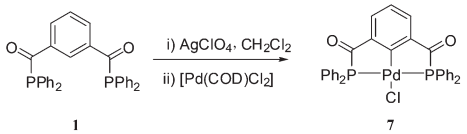

Scheme 4

In the ^1H NMR spectrum of **7**, disappearance of the signal due to the *ipso*-proton around 8.50 ppm confirms the Pd–C bond formation through the elimination of $HClO_4$. The structure of **7** has been confirmed by single crystal X-ray analysis.

Another convenient method for the synthesis of pincer complexes is the oxidative addition of bromo- or iodo derivative to low-valent metal precursors. Thus the reaction between bromo-functionalized bis(phosphomide) **2** and $[Ni(COD)_2]$ in THF yielded the pincer complex, $[NiBr\{2,6\text{-}\{Ph_2PC(O)\}_2(C_6H_3)\}]$ (**8**), while a similar reaction between **2** and $[Pd_2(dba)_3]$ gave $[PdBr\{2,6\text{-}\{Ph_2PC(O)\}_2(C_6H_3)\}]$ (**9**) in good yield (Scheme 5). The $^{31}P\{^1H\}$ NMR spectra of complexes **8** and **9** show single resonances at 49.6 and 52.2 ppm, respectively.

Synthesis of group 11 metal complexes

Bis(phosphomide) **1**, on treatment with cuprous halides (CuX, X = Cl, Br, I), yielded the binuclear complexes $[Cu_2(\mu\text{-}X)_2\{1,3\text{-}\{Ph_2PC(O)\}_2(C_6H_4)\}_2]$ (**10**, X = Cl; **11**, X = Br; **12**, X = I) containing rhombic Cu_2X_2 units as shown in Scheme 6. All the complexes were highly soluble in most of the organic solvents. The $^{31}P\{^1H\}$ NMR spectra of complexes **10–12** show single resonances at 4.0, 1.9 and 1.3 ppm, respectively. Treatment of **1** with $[Cu(NCCH_3)_4]BF_4$ in a 1 : 1 ratio afforded the tetrahedral cationic complex, $[Cu(NCCH_3)_2\{1,3\text{-}\{Ph_2PC(O)\}_2(C_6H_4)\}]BF_4$ (**13**). The $^{31}P\{^1H\}$ NMR spectrum of complex **13** shows a single resonance at 10.5 ppm. The reaction of **1** with $AgClO_4$ in a

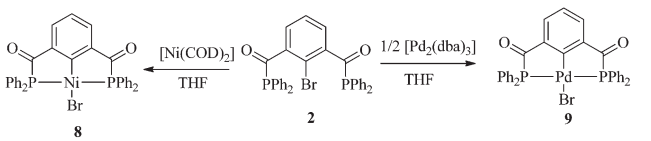

Scheme 5

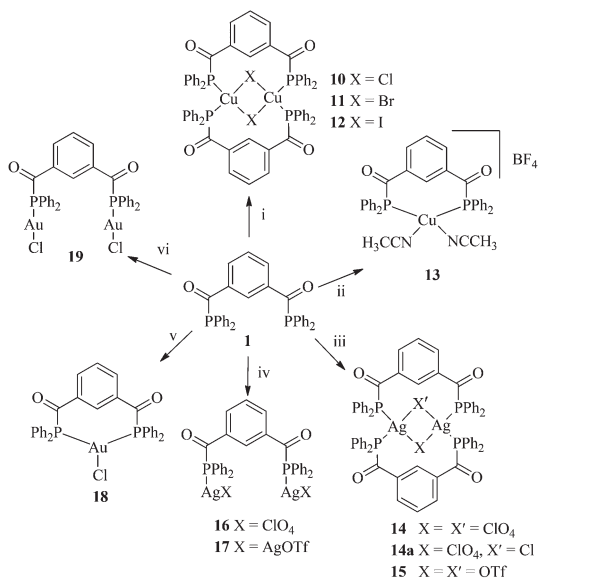

Scheme 6 (i) CuX, CH_3CN/CH_2Cl_2, (ii) $[Cu(CH_3CN_4]BF_4$, CH_2Cl_2, (iii) AgX, THF, (iv) 2AgX, THF, (v) $[AuCl(SMe_2)]$, CH_2Cl_2, and (vi) $2[AuCl(SMe_2)]$, CH_2Cl_2.

1 : 1 molar ratio followed by crystallization from dichloromethane/hexane resulted in the formation of a binuclear complex, $[Ag_2(\mu\text{-}ClO_4)_2\{1,3\text{-}\{Ph_2PC(O)\}_2(C_6H_4)\}_2]$ (**14**), which was contaminated with a trace (~4%) amount of $[Ag_2(\mu\text{-}Cl)(\mu\text{-}ClO_4)\{1,3\text{-}\{Ph_2PC(O)\}_2(C_6H_4)\}_2]$ (**14a**) which gave single crystals suitable for X-ray diffraction study. The presence of a bridging chloride ion is due to the presence of a trace amount of AgCl found in $AgClO_4$. However, attempts to grow crystals of **14** suitable for single crystal X-ray diffraction studies have been unsuccessful. A similar reaction between bis(phosphomide) **1** and AgOTf in a 1 : 1 molar ratio yielded the complex $[Ag_2(\mu\text{-}OTf)_2\{1,3\text{-}\{Ph_2PC(O)\}_2(C_6H_4)\}_2]$ (**15**) in good yield.

The bis(phosphomide) **1** on treatment with 2 equiv. of AgX (X = ClO_4, OTf) produced binuclear complexes, $[Ag_2X_2\{1,3\text{-}\{Ph_2PC(O)\}_2(C_6H_4)\}]$ (**16**, X = ClO_4; **17**, X = OTf), in good yield. Complexes **16** and **17** are colorless solids which are highly light-sensitive in solution but moderately stable in the solid state. The $^{31}P\{^1H\}$ NMR spectra of complexes **14–17** show broad resonances at 15.8, 14.8, 19.7 and 18.8 ppm, respectively. The unresolved broad resonances are due to the presence of two isotopes of silver (^{109}Ag (48%) and ^{107}Ag (52%)) almost in equal proportions. However, in the case of silver complex **17**, the $^{31}P\{^1H\}$ NMR spectrum recorded at −40 °C showed two doublets centered at 18.8 ppm with $^1J_{^{109}AgP}$ and $^1J_{^{107}AgP}$ couplings of 730.5 and 641.4 Hz, respectively. The 1 : 1 reaction between **1** and $[AuCl(SMe_2)]$ in dichloromethane gave $[AuCl\{1,3\text{-}\{Ph_2PC(O)\}_2(C_6H_4)\}]$ (**18**) while a similar reaction of **1** with two equivalents of $AuCl(SMe_2)$ afforded a binuclear complex $[Au_2Cl_2\{1,3\text{-}\{Ph_2PC(O)\}_2(C_6H_4)\}]$ (**19**) with ligand **1** exhibiting the bridged bidentate mode of coordination. The $^{31}P\{^1H\}$ NMR spectra of complexes **18** and **19** exhibit single resonances at 22.2 and 31.4 ppm, respectively.

Molecular structures of complexes 5, 7–10, 12, and 14a

Perspective views of the molecular structures of complexes **5**, **7–10**, **12** and **14a** with atom numbering schemes are shown in Fig. 1–7. Selected bond distances and bond angles are listed in Tables 1 and 3 and crystallographic data and the details of the structure determinations are given in Table 4.

In the molecular structure of **5** the ligand coordinates to the ruthenium centers in a bridging fashion. The ruthenium atoms adopt pseudo octahedral geometries with the *p*-cymene coordinating in a typical η^6 fashion. The C23–P1–Ru1 and

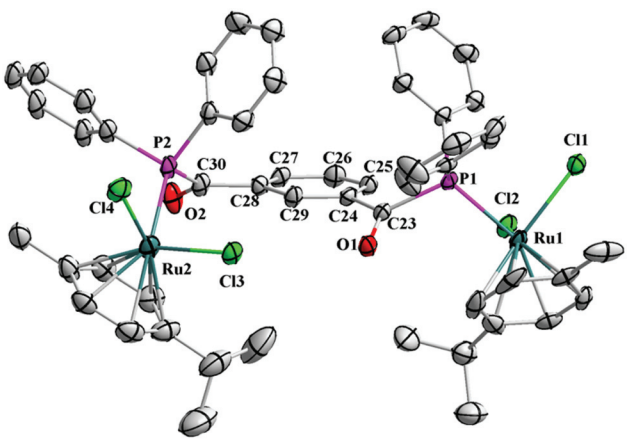

Fig. 1 Molecular structure of $[Ru_2(\eta^6\text{-}p\text{-cymene})_2Cl_4\{1,3\text{-}\{Ph_2PC(O)\}_2(C_6H_4)\}]$ (**5**). All hydrogen atoms have been omitted for clarity. Thermal ellipsoids are drawn at a 50% probability level.

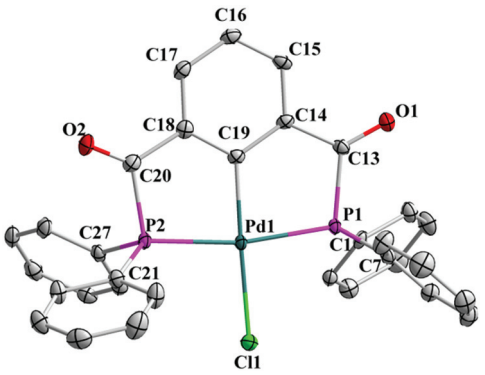

Fig. 2 Molecular structure of the complex $[PdCl\{2,6\text{-}\{Ph_2PC(O)\}_2(C_6H_3)\}]$ (**7**). All hydrogen atoms have been omitted for clarity. Thermal ellipsoids are drawn at a 50% probability level.

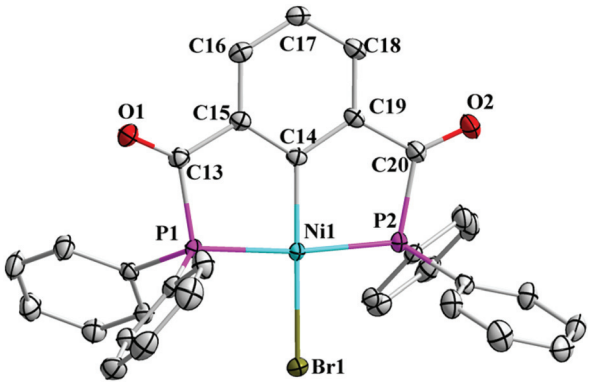

Fig. 3 Molecular structure of $[NiBr\{2,6\text{-}\{Ph_2PC(O)\}_2(C_6H_3)\}]$ (**8**). All hydrogen atoms have been omitted for clarity. Thermal ellipsoids are drawn at a 50% probability level.

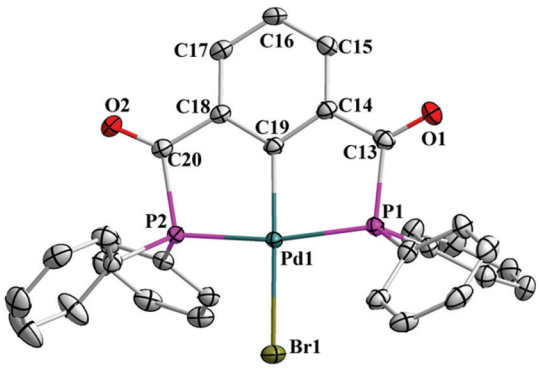

Fig. 4 Molecular structure of $[PdBr\{2,6\text{-}\{Ph_2PC(O)\}_2(C_6H_3)\}]$ (**9**). All hydrogen atoms have been omitted for clarity. Thermal ellipsoids are drawn at a 50% probability level.

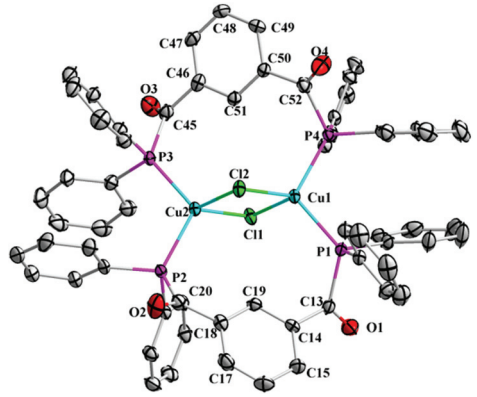

Fig. 5 Molecular structure of $[Cu_2(\mu\text{-}Cl)_2\{1,3\text{-}\{Ph_2PC(O)\}_2(C_6H_4)\}_2]$ (**10**). All hydrogen atoms have been omitted for clarity. Thermal ellipsoids are drawn at a 50% probability level.

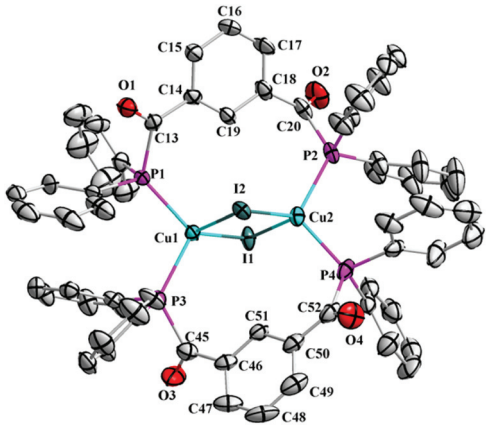

Fig. 6 Molecular structure of $[Cu_2(\mu\text{-}I)_2\{1,3\text{-}\{Ph_2PC(O)\}_2(C_6H_4)\}_2]$ (**12**). All hydrogen atoms have been omitted for clarity. Thermal ellipsoids are drawn at a 50% probability level.

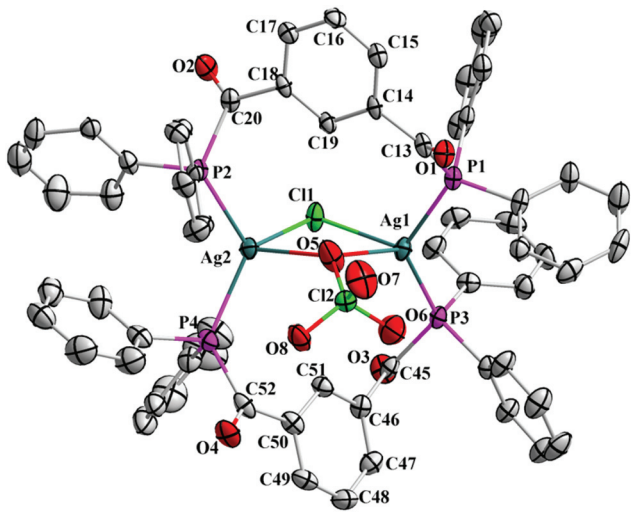

Fig. 7 Molecular structure of $[Ag_2(\mu\text{-}ClO_4)(\mu\text{-}Cl)\{1,3\text{-}\{Ph_2PC(O)\}_2(C_6H_4)\}_2]$ (**14a**). All hydrogen atoms have been omitted for clarity. Thermal ellipsoids are drawn at a 50% probability level.

C30–P2–Ru2 bond angles (Table 1) are significantly different, a feature which is likely to be due to packing considerations. The Cl1–Ru1–Cl2 and Cl3–Ru2–Cl4 bond angles are slightly different but compare well with the reported range of Cl–Ru–Cl bond angles (86.27–89.77°) for analogous ruthenium *p*-cymene complexes.[25] The P1–C23 and P2–C30 bond lengths are equal within experimental error as are the Ru1–P1 and Ru2–P2 bond distances (Table 1). There appears to be a weak C–H···π interaction between C34 and H34 and the phenyl ring based on C11 at $1-x$, $1-y$, $-z$ (H34···ring centroid = 2.83 Å, C34–H34···ring centroid = 153°).

In the molecular structures of nickel and palladium complexes **8**, **7** and **9**, the ligand binds to the metal in a typical terdentate fashion. Bond distances and bond angles of some related nickel and palladium pincer complexes along with those of complexes **7–9** are given in Table 2. Notably, complexes **7–9** show larger P–Ni–P (172.80(3)°) and P–Pd–P (169.15(3) and 168.56(2)°) bond angles than the corresponding complexes of PCP and POCOP ligands. This may be due to the longer P–C(O) bond distances in complexes **7–9** as compared to the relatively shorter P–C and P–O bond distances in the corresponding PCP and POCOP pincer complexes. The Ni–C14 and Pd–C19 bond lengths (Table 1) compare well with the reported range of 1.87–1.90 Å for nickel and 1.99–2.03 Å for palladium complexes.[26,27] The two five-membered chelate rings are coplanar. The P1–C13–C15 and P2–C20–C19 bond angles for **8** and the P1–C13–C14 and P2–C20–C18 bond angles for **9** (Table 1) are considerably different from the P–C–C bond angles in PCP type pincer complexes but are close to the P–O–C bond angles found in POCOP type pincer complexes (Table 2). On the other hand, the M–P–C bond angles in **7–9** are within the range observed in similar pincer complexes (Table 2). Complex **8** shows two weak C–H···O and one C–H···π interactions but **9** shows only the latter.

The molecular structures of copper complexes, **10** and **12**, show binuclear units in which the metals are coordinated by two phosphorus atoms and two halide ions in a distorted tetrahedral arrangement. The bis(phosphomides) act as bridging ligands coordinating to two different copper centers. The copper atoms are also linked by the halides so that the core of the complex is a rhomboid with Cu–Cu and X–X diagonals. As is evident from Fig. 4 and 5, the Cu_2X_2 core is almost perpendicular to the plane formed by the four coordinating phosphorus atoms. The P–C(O) bond distances for complexes **10** and **12** are in the range 1.8803(38) to 1.9054(61) Å while the Cu–P bond distances in **10** are slightly shorter than those in **12** (Table 3). The Cu···Cu distances are 3.1684(8) and 3.2361(8) Å, respectively, for **10** and **12** while the bond angles Cl1–Cu1–Cl2 and Cl1–Cu2–Cl2 are 96.35(3)° and 96.14(3)° for complex **10** and for complex **12** the bond angles I1–Cu1–I2 and I1–Cu2–I2 are 105.165(20)° and 105.376(20)°. Similar to complexes **10** and **12** the molecular structure of **14a** also shows the presence of two bridging ligands and a discrete core of two tetrahedrally coordinated silver(I) centers with bridging perchlorate and chloride ions. The PCP ligand, $1,3\text{-}C_6H_4(CH_2PPh_2)_2$, is also

Table 1 Selected bond distances (Å) and bond angles (°) for **5** and **7–9**[a]

Compound **5**		Compound **7**		Compound **8**		Compound **9**	
Bond length (Å)		Bond length (Å)		Bond length (Å)		Bond length (Å)	
Ru1–P1	2.3505(13) (2.387)	Pd1–C19	2.030(3) (2.049)	Ni1–C14	1.923(2) (1.946)	Pd1–C19	2.039(2) (2.057)
Ru2–P2	2.3554(13) (2.389)	Pd1–P1	2.2651(9) (2.328)	Ni1–P1	2.1611(6) (2.222)	Pd1–P2	2.2744(10) (2.327)
Ru1–Cl1	2.4207(14) (2.441)	Pd1–P2	2.2763(9) (2.328)	Ni1–P2	2.1704(6) (2.222)	Pd1–P1	2.2826(10) (2.327)
Ru1–Cl2	2.4012(12) (2.434)	Pd1–Cl1	2.3590(10) (2.416)	Ni1–Br1	2.3315(4) (2.378)	Pd1–Br1	2.4828(10) (2.528)
Ru2–Cl3	2.4131(13) (2.447)	P1–C13	1.881(4) (1.90)	P1–C13	1.882(2) (1.898)	P1–C13	1.889(2) (1.903)
Ru2–Cl4	2.4057(16) (2.414)	P2–C20	1.881(4) (1.90)	P2–C20	1.876(2) (1.898)	P2–C20	1.888(2) (1.903)
P1–C23	1.892(4) (1.909)	C13–O1	1.216(4) (1.220)	O1–C13	1.212(3) (1.218)	O1–C13	1.212(3) (1.219)
P2–C30	1.881(5) (1.962)	C20–O2	1.205(5) (1.220)	O2–C20	1.212(3) (1.218)	O2–C20	1.211(3) (1.219)
O1–C23	1.206(5) (1.227)						
O2–C30	1.227(6) (1.211)						
Bond angle (°)		Bond angle (°)		Bond angle (°)		Bond angle (°)	
P1–Ru1–Cl2	90.03(5) (89.97)	P1–Pd1–P2	169.15(3) (168.74)	P1–Ni1–P2	172.80(3) (172.73)	P2–Pd1–P1	168.56(2) (168.57)
P1–Ru1–Cl1	86.12(4) (87.74)	C19–Pd1–Cl1	177.42(10) (180.00)	C14–Ni1–Br1	175.11(7) (179.97)	C19–Pd1–Br1	177.22(6) (179.96)
P2–Ru2–Cl3	96.40(4) (84.49)	C14–C13–P1	111.0(2) (111.89)	C15–C13–P1	109.10(15) (109.89)	C18–C20–P2	111.00(15) (111.92)
P2–Ru2–Cl4	83.79(4) (86.79)	C18–C20–P2	111.1(2) (111.89)	C19–C20–P2	109.66(16) (109.89)	C14–C13–P1	111.01(16) (111.92)
O1–C23–P1	117.9(3) (115.60)	C13–P1–Pd1	102.45(11) (101.33)	C13–P1–Ni1	103.11(8) (101.52)	C13–P1–Pd1	102.39(8) (101.33)
O2–C30–P2	119.1(3) (111.85)	C20–P2–Pd1	102.29(12) (101.33)	C20–P2–Ni1	102.52(8) (101.52)	C20–P2–Pd1	102.10(7) (101.33)
C23–P1–Ru1	111.26(14) (107.10)						
C30–P2–Ru2	107.22(15) (116.01)						
C24–C23–P1	121.5(3) (123.47)						
C28–C30–P2	121.6(3) (127.51)						

[a] The optimized geometrical parameters obtained at the B3LYP/6-31G**, SDD level of theory are provided in parentheses below the corresponding values obtained from X-ray crystallographic analyses.

reported to form a similar type of Ag(I) complexes.[28] The average P–C(O) bond distance in **14a** is comparable to those in **10** and **12** while the Ag–P bond distances range from 2.4246(15) to 2.4533(13) Å (Table 3). The perchlorate ion coordinates in an asymmetric bridged monodentate fashion to both silver atoms with Ag1–O5 and Ag2–O5 bond lengths of 2.707(5) and 2.529(4) Å, respectively. All the three complexes show weak C–H···O interactions.

Hydroformylation of alkenes

The utility of bisphosphomides in homogeneous catalysis is not known. However, the catalytic activity of a few monophosphomides ligands have been investigated in the rhodium catalyzed hydroformylation of alkenes.[19g] The hydroformylation of hex-1-ene was studied as a test reaction for evaluating the catalytic utility of **1**. The reactions were performed at 60 °C with a 2 : 1 ratio of ligand **1** and [Rh(acac)(CO)$_2$], and the formation of the products was determined by gas chromatography. Initially, the reaction was studied at different syngas (CO/H$_2$) pressures in the range of 10–30 bar (Table 5, entries 1–3) where 30 bar was found to provide the maximum conversion and selectivity of the desired product. Surprisingly, with a decrease in catalyst loading the regioselectivity towards the linear aldehyde was increased and a l : b ratio of 2.3 was achieved (Table 5, entry 5).

Further the catalytic activity of the bisphosphomide **1** was investigated in the hydroformylation of styrene. Styrene has a

Table 2 Selected bond lengths (Å) and bond angles (°) for nickel and palladium pincer complexes with ligands of the type $R_2PYCYPR_2$ (Y = C(O), CH_2, O; R = Ph, Cy, ^{t}Bu)

No.	Metal	X	Y	R	M–C	M–X	P–M	P–Y	P–M–P	M–P–Y	P–Y–C
1	Ni	Br	C(O)	Ph	1.923	2.3315	2.1611	1.882	172.80	103.11	109.10[a]
							2.1704	1.876		102.52	109.66
2	Ni	Br	CH_2	Ph	1.920	2.3290	2.177	1.814	165.3	102.9	103.1[26a]
							2.173	1.821		102.5	104.0
3	Ni	Br	CH_2	Cy	1.909	2.360	2.168	1.824	167.6	103.6	108.3[26b]
							2.185	1.817		105.0	105.6
4	Ni	Br	O	Ph	1.874	2.3002	2.1544	1.649	164.39	106.15	111.51[26c]
							2.1550	1.648		106.54	111.26
5	Ni	Cl	O	Ph	1.879	2.1880	2.1556	1.6462	164.16	106.46	111.43[26d]
							2.1582	1.6441		105.94	111.74
6	Ni	I	O	Ph	1.890	2.4976	2.1553	1.6486	164.20	106.67	111.50[26e]
							2.1601	1.6488		106.42	111.67
7	Pd	Br	C(O)	Ph	2.039	2.4828	2.2826	1.889	168.56	102.10	111.00[a]
							2.2744	1.888		102.17	111.01
8	Pd	Cl	C(O)	Ph	2.030	2.3590	2.2651	1.881	169.15	102.45	109.10[a]
							2.2763	1.881		102.29	109.66
9	Pd	Br	CH_2	Ph	2.027	2.495	2.292	1.833	162.5	101.8	105.1[26a]
							2.287	1.826		101.6	106.2
10	Pd	Br	CH_2	^{t}Bu	2.022	2.5534	2.318	1.843	166.88	101.6	110.1[27a]
							2.325	1.818		101.6	110.1
11	Pd	Cl	CH_2	Ph	1.998	2.367	2.228	1.815	162.0	101.04	105.7[27b]
							2.294	1.824		101.3	105.4
12	Pd	Cl	CH_2	Cy	2.012	2.427	2.226	1.826	165.5	102.6	111.2[27c]
							2.294	1.824		104.1	108.6

[a] This work.

preference for the formation of branched aldehyde, due to the formation of a stable η^3-benzylic-rhodium complex.[29a,b] At 30 bar pressure, the hydroformylation of styrene showed 96% conversion with good regioselectivity towards the branched aldehyde (Table 6, entry 1). Encouraged by the high activity and selectivity, a series of substituted styrenes were then hydroformylated to investigate the viability of the process. A slight increase in the regioselectivity towards the branched aldehyde was observed with electron withdrawing substituents on the phenyl ring.[29c] It was found that the electron-donating substituents on styrene gave higher conversion than those with electron-withdrawing substituents (Table 6, entries 2–5).[30] Allyl anisole formed three structural aldehydes due to the isomerisation reaction. Thus, under mild conditions, higher selectivity, good regioselectivity and moderate turnover numbers were obtained in the hydroformylation of styrenes. The rhodium complex generated *in situ* during the hydroformylation reaction has the composition, [Rh(acac)(η^2-bisphosphomide)] (no C–H activation was observed to form a pincer complex). The $^{31}P\{^1H\}$ NMR spectrum of the complex shows a doublet at 62.8 ppm with a $^1J_{RhP}$ coupling of 149 Hz. In the absence of ligand, the conversions were in the range of 30–40% and 20–30%, for styrene derivatives and hex-1-ene, respectively.

Density functional theory studies

We have performed density functional theory studies using the B3LYP/6-31G**, SDD level of theory in order to gain additional insights into the structure and bonding of the pincer complexes. The geometric comparisons for compounds **5**, **7–10**, **12** and **14a**, as provided in Tables 1 and 3, indicate that the agreement between the computed geometric parameters and those obtained using the X-ray crystallographic methods is generally good.[31] An additional analysis of the orbital interactions responsible for the bonding pattern for a representative pincer complex [PdBr{2,6-{$Ph_2PC(O)$}$_2$(C_6H_3)}] (**9**) was carried out using the Natural Bonding Orbital (NBO) method using the optimized geometries at the B3LYP/6-31G**, SDD level of theory. The atomic orbital contributions to the important molecular orbitals were examined using the AOMix procedure. The key results are summarized in the following sections.

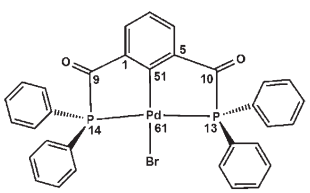

The AOMix analysis, as summarized in Table 7, reveals that the HOMO and LUMO are primarily located on the pincer ligand (PCP) fragment. In particular, LUMO exhibits an exclusive contribution by the pincer backbone while a small contribution from palladium is evident in the HOMO. The orbital interactions responsible for strong stabilizing interaction between the phosphorus and palladium are noticeable with a more than 80% contribution from phosphorus to such orbitals. For instance, HOMO − 35 has an overwhelming contribution from

Table 3 Selected bond distances (Å) and bond angles (°) for complexes **10**, **12** and **14a**

Compound **10**		Compound **12**		Compound **14a**	
Bond length (Å)		Bond length (Å)		Bond length (Å)	
P2–Cu2	2.2616(12) (2.332)	P3–Cu1	2.2871(14) (2.370)	Ag1–P1	2.4506(14) (2.519)
P3–Cu2	2.2579(11) (2.333)	P1–Cu1	2.2882(14) (2.356)	Ag2–P2	2.4368(13) (2.519)
P1–Cu1	2.2584(11) (2.327)	P4–Cu2	2.2891(16) (2.351)	Ag1–P3	2.4533(13) (2.517)
P4–Cu1	2.2594(12) (2.357)	P2–Cu2	2.2794(14) (2.357)	Ag2–P4	2.4246(15) (2.519)
Cu1–Cl1	2.3908(11) (2.437)	Cu1–I1	2.6750(7) (2.881)	Ag1–Cl1	2.5868(13) (2.664)
Cu1–Cl2	2.3522(11) (2.428)	Cu1–I2	2.6613(7) (2.754)	Ag2–Cl1	2.5189(13) (2.617)
Cu2–Cl1	2.3931(11) (2.482)	Cu2–I1	2.6852(7) (2.761)	Ag1–O5	2.707(5) (2.564)
Cu2–Cl2	2.3578(11) (2.489)	Cu2–I2	2.6435(7) (2.894)	Ag2–O5	2.529(4) (2.538)
C20–O2	1.2054(54) (1.218)	C45–O3	1.207(6) (1.215)		
Bond angle (°)		Bond angle (°)		Bond angle (°)	
C20–P2–Cu2	116.18(15) (111.43)	C45–P3–Cu1	122.03(16) (124.28)	P1–Ag1–P3	129.12(5) (132.61)
C45–P3–Cu2	123.67(14) (124.18)	C52–P4–Cu2	120.35(18) (122.52)	P4–Ag2–P2	121.15(5) (123.58)
C13–P1–Cu1	122.39(14) (126.97)	C13–P1–Cu1	120.75(18) (126.07)	Cl1–Ag1–O5	82.44(9) (88.52)
C52–P4–Cu1	116.82(15) (121.65)	C20–P2–Cu2	122.22(15) (111.85)	Cl1–Ag2–O5	87.48(12) (90.09)
P2–Cu2–Cl1	111.44(4) (109.85)	P3–Cu1–I1	106.21(4) (93.90)	Ag2–Cl1–Ag1	94.81(4) (88.68)
P1–Cu1–Cl1	108.35(4) (118.76)	P4–Cu2–I1	112.58(4) (111.99)	Ag2–O5–Ag1	91.70(16) (92.69)
				C20–P2–Ag2	116.49(16) (128.40)
				C13–P1–Ag1	121.81(16) (120.81)
				C14–C13–P1	118.1(3) (119.08)

the phosphorus orbital. The relative contributions to the molecular orbitals are pictorially represented using orbital contour diagrams in Fig. 8.

Conclusions

The transition metal chemistry of bis(phosphomide) ligands is described. The transmetallation reaction afforded palladium(II) pincer complex under mild conditions. The nickel and palladium pincer complexes were also obtained *via* oxidative addition of bromo-functionalized bis(phosphomide) ligand to nickel(0) and palladium(0) metal reagents. Although both the ligands are sensitive to moisture, the metal complexes are moderately stable but on prolonged exposure they decompose; a palladium complex, being more sensitive, readily gives palladium black. The *in situ* generated rhodium(I) complex containing bis(phosphomide) ligand catalyses the hydroformylation of styrenes and hex-1-ene with moderate selectivity. The DFT calculations have hinted at the overall electron contributions towards HOMO and LUMO from both metal and donor atoms. This information about the overall electron density present at the metal center can eventually assist in understanding their catalytic behavior in various organic transformations. Further work in this direction is in progress.

Experimental

General procedures

All manipulations were performed using standard vacuum-line and Schlenk techniques under a nitrogen atmosphere unless otherwise stated. All of the solvents were purified by conventional procedures[32] and distilled prior to use. The compounds CuCl,[33] CuBr,[33] $[Cu(CH_3CN)_4]BF_4$,[34] $[AuCl(SMe_2)]$,[35] $[Ru(\eta^6\text{-}p\text{-cymene})Cl_2]_2$,[36] $[Pd(\eta^3\text{-}C_3H_5)Cl]_2$ [37] and $[Pd_2dba_3]$[38] were prepared according to the published procedures. The metal precursors CuI, AgOTf, $AgClO_4$ and $[Ni(COD)_2]$ were purchased from Aldrich Chemicals and used as received. Other chemicals were obtained from commercial sources and purified prior to use.

Table 4 Crystallographic information for compounds **5**, **7–9**, **11**, **12** and **14a**

	5	7	8	9	10	12	14a
Formula	$C_{53}H_{54}Cl_6O_2P_2Ru_2$	$C_{33}H_{25}Cl_3O_2P_2Pd$	$C_{33}H_{25}BrCl_2NiO_2P_2$	$C_{32}H_{23}BrO_2P_2Pd$	$C_{72}H_{60}Cu_2Cl_2N_4O_4P_4$	$C_{68}H_{56}Cu_2I_2O_5P_4$	$C_{131}H_{102}Ag_4Cl_{10}O_{16}P_8$
Fw	1199.74	728.28	724.99	687.75	1367.10	1457.89	2965.86
Crystal system	Triclinic	Triclinic	Triclinic	Monoclinic	Triclinic	Monoclinic	Monoclinic
Space group	$P\bar{1}$	$P\bar{1}$	$P\bar{1}(2)$	$P2(1)/n$	$P\bar{1}$	$P2(1)/n$	$P2(1)/n$
a (Å)	11.277(4)	11.789(3)	11.9842(12)	9.112(4)	14.1567(18)	13.0999(19)	14.296(3)
b (Å)	12.280(4)	12.147(2)	12.0194(12)	24.206(11)	14.4395(18)	29.083(4)	29.654(7)
c (Å)	21.270(7)	12.8117(19)	12.7559(13)	12.977(6)	17.487(2)	18.143(3)	15.474(3)
α (°)	95.437(4)	62.959(14)	63.683(1)	90.00	91.137(2)	90.00	90.00
β (°)	91.368(4)	68.313(17)	67.267(1)	102.137(6)	91.028(2)	110.317(2)	102.318(3)
γ (°)	92.086(4)	76.844(18)	76.562(1)	90.00	112.604(2)	90.00	90.00
V (Å^3)	2929(17)	1514.5(5)	1514.9(3)	2798(2)	3298.1(7)	6482.3(16)	6409(2)
Z	2	2	2	4	2	4	2
ρ_{calc} (g cm^{-3})	1.360	1.551	1.589	1.632	1.377	1.494	1.537
μ (MoKα) (mm^{-1})	0.879	0.850	2.272	2.234	0.875	1.755	0.973
F (000)	1216	712	732	1368	1408	2912	2988
Crystal size (mm)	0.26 × 0.15 × 0.08	0.59 × 0.30 × 0.28	0.26 × 0.09 × 0.16	0.18 × 0.17 × 0.10	0.24 × 0.19 × 0.13	0.22 × 0.10 × 0.05	0.21 × 0.11 × 0.09
T (K)	100(2)	100(2)	100(2)	100(2)	100(2)	100(2)	100(2)
2θ range (°)	2.41–28.09	3.20–25.40	2.23–29.10	2.44–28.64	2.41–28.09	2.36–27.94	2.19–27.06
Total no. of reflns	43808	10831	26273	48179	43808	54692	53590
No. of indep. reflns	12820	5269	7237	7136	12820	14289	14041
R_1	0.0594	0.0458	0.0354	0.0283	0.0594	0.0446	0.0565
wR_2	0.1568	0.1250	0.1031	0.1141	0.1568	0.1031	0.1435
GOF (F^2)	1.048	1.042	1.059	1.019	1.048	1.059	1.021

Table 5 Hydroformylation of hex-1-ene with bisphosphomide **1**

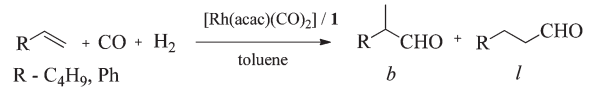

Entry	Ligand	CO/H_2(Bar)	Conversion	$l:b$	TON
1	**1**	10	31	1.5	620
2	**1**	20	66	1.4	1080
3	**1**	30	81	1.5	1776
4	**1**	30[a]	68	1.4	3400
5	**1**	30[b]	52	2.3	5200

Time = 4 h, temp. = 60 °C, solvent = toluene. S/C = 2000, isomerised alkenes were not detected. [a] S/C = 5000. [b] S/C = 10 000.

Table 6 Hydroformylation of styrene and its derivatives

Entry	Substrate	Conversion	$b:l$	% b	TON
1	Styrene	96	2.2	69	1920
2	4-*tert*-Butylstyrene	98.5	2.9	74	1970
3	4-Methyl styrene	99	2.2	68	1980
4	4-Cl-styrene	66	2.7	73	1320
5	4-Br-styrene	77.6	2.6	72	1553
6	4-Allyl anisole[a]	92.6	1.58	46	1852

Time = 4 h, temp. = 60 °C, P = 30 bar (1 : 1, CO : H_2), solvent = toluene, S/C = 2000. [a] Isomerised aldehyde = 24%.

Table 7 Composition[a] and energies of important Kohn–Sham orbitals of palladium pincer complex **9** obtained using the wave function generated at the B3LYP/6-31G**, SDD level of theory

Orbital	Energy (eV)	Orbital character
LUMO + 2	−2.072	12.67% Pd d_{z^2}, 87.32% PCP
LUMO	−2.600	100% PCP
HOMO	−3.164	11.56% Pd d_{yz}, 88.44% P P_x
HOMO − 1	−6.498	2.72% Pd d_{xz}, 97.28% PCP
HOMO − 2	−6.874	0.51% Pd d_{yz}, 99.49% PCP
HOMO − 18	−9.500	0.11% Pd d_{xz}, 99.9% C P_y
HOMO − 35	−11.42	11.76% Pd $d_{x^2-y^2}$, 88.24% P P_x
HOMO − 36	−11.55	1.30% Pd d_{z^2}, 98.69% P P_y
HOMO − 38	−11.63	2.7% Pd S, 97.30% C P_z

[a] PCP pincer and Pd–Br are considered as two interacting partners in AOMix analysis. The contributions listed as coming from palladium are inclusive of those of bromine.

Instrumentation

The NMR spectra were recorded at the following frequencies: 400 MHz (^{1}H), 100 MHz (^{13}C), 162 MHz (^{31}P) using either a Varian VXR 400 or a Bruker AV 400 spectrometer. ^{13}C and ^{31}P NMR spectra were acquired using broad band decoupling. The spectra were recorded in $CDCl_3$ solutions with $CDCl_3$ as an internal lock; chemical shifts of ^{1}H and ^{13}C NMR spectra are reported in ppm downfield from TMS, used as an internal standard. The chemical shifts of $^{31}P\{^1H\}$ NMR spectra are referred to 85% H_3PO_4 as an external standard. The microanalyses were performed using a Carlo Erba Model 1112 elemental

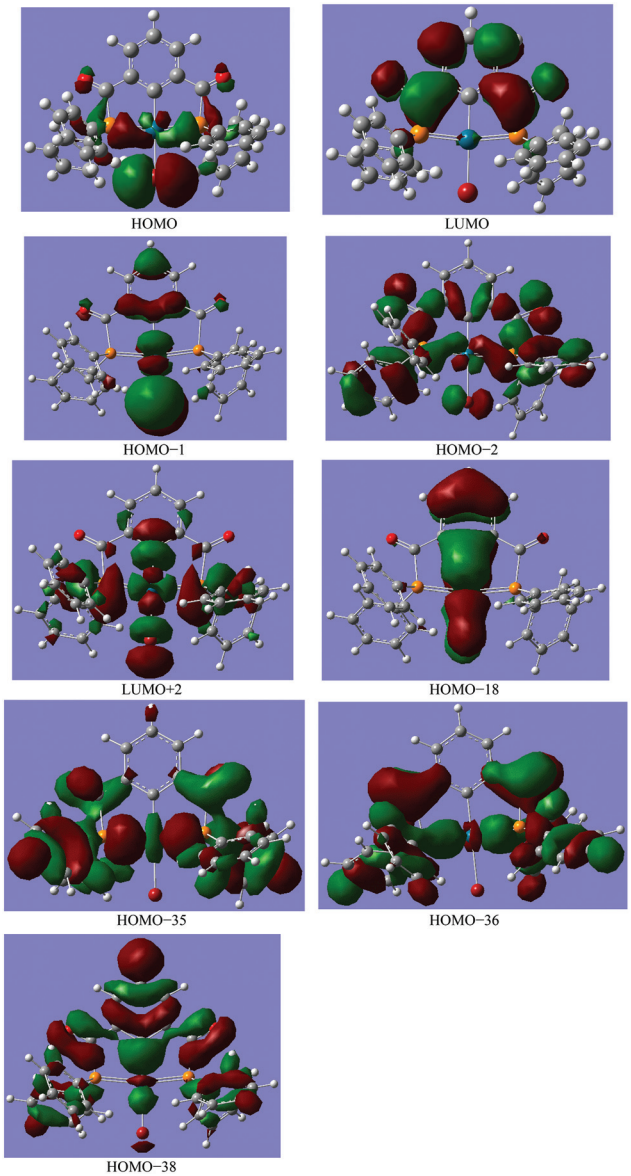

Fig. 8 Selected set of Kohn–Sham orbital contours for key orbitals of Pd-pincer complex **9**.

analyzer. Mass spectra were recorded using a Waters Q-Tof micro (YA-105). The melting points were observed in capillary tubes and are uncorrected.

Synthesis of 1,3-{$Ph_2PC(O)$}$_2(C_6H_4)$ (1)

A solution of isophthaloyl chloride (2.0 g, 9.85 mmol) in 15 mL diethyl ether was added dropwise over 10 minutes to a solution of diphenylphosphine (3.6 g, 19.7 mmol) in diethyl ether (40 mL) at 0 °C in the presence of Et_3N (1.9 g, 2.7 mL, 19.7 mmol). The color of the solution immediately turned yellow. The reaction mixture was stirred for 3 h at room temperature and the amine hydrochloride was removed by filtration. The solvent was removed under reduced pressure to give **1** as a yellow-orange solid. Yield: 94% (4.60 g). Mp: 99–101 °C. Anal. Calcd for $C_{32}H_{24}O_2P_2$: C, 76.49; H, 4.81. Found: C, 76.42; H, 4.78. FT IR (KBr disc) cm^{-1}: ν_{CO}: 1649 s. ^1H NMR (400 MHz, $CDCl_3$): δ 8.58 (t, 1H, Ar, $^4J_{HH}$ = 1.8 Hz), 7.99 (d, 2H, Ar, $^3J_{HH}$ = 7.7 Hz), 7.44–7.29 (m, 21H, Ar). $^{31}P\{^1H\}$ NMR (162 MHz, $CDCl_3$): δ 12.3 (s).

Synthesis of 2-Br-1,3-{$Ph_2PC(O)$}$_2C_6H_3$ (2)

To a solution of diphenylphosphine (0.66 g, 3.547 mmol) in diethyl ether (20 mL) at 0 °C was added a solution of 2-bromoisophthaloyl chloride (0.50 g, 1.773 mmol) in the same solvent (10 mL) in the presence of Et_3N (0.358 g, 0.49 mL, 3.547 mmol). The color of the solution immediately turned yellow. The reaction mixture was stirred for 3 h at room temperature. The amine hydrochloride was removed by filtration and the solvent was removed under reduced pressure to give a yellow solid. The solid was dissolved in 5 mL of CH_2Cl_2 and saturated with 6 mL of hexane and stored at −20 °C to give an analytically pure **2** as a yellow solid. Yield: 95% (0.979 g). Mp: 112–114 °C. Anal. Calcd for $C_{32}H_{23}BrO_2P_2$: C, 66.11; H, 3.99. Found: C, 66.19; H, 3.83. FT IR (KBr disc) cm^{-1}: ν_{CO}: 1649 s. ^1H NMR (400 MHz, $CDCl_3$): δ 7.42–7.59 (m, 8H, Ar), 7.37–7.29 (m, 14H, Ar), 7.09 (t, 1H, Ar, $^3J_{HH}$ = 7.6 Hz). $^{31}P\{^1H\}$ NMR (162 MHz, $CDCl_3$): δ 21.1 (s).

Synthesis of 1,3-{$Ph_2P(S)C(O)$}$_2(C_6H_4)$ (3)

A mixture of **1** (0.1 g, 0.198 mmol) and elemental sulfur (0.013 g, 0.417 mmol) in diethyl ether (12 mL) was stirred vigorously for 3 h at room temperature. The bis(sulfide) derivative precipitated out as a yellow solid which was filtered off and washed with 10 mL of diethyl ether. The solid was dissolved in THF followed by filtration to remove unreacted sulfur. The yellow filtrate obtained was dried under reduced pressure to yield **3** as a yellow solid. Yield: 60% (0.067 g). Mp: 124–126 °C. Anal. Calcd for $C_{32}H_{24}O_2P_2S_2$: C, 67.83; H, 4.27; S, 11.32. Found: C, 67.49; H, 4.23; S, 10.86. FT IR (KBr disc) cm^{-1}: ν_{CO}: 1656 s. ^1H NMR (400 MHz, $CDCl_3$): δ 8.51 (s, 1H, Ar), 8.10 (d, 2H, Ar, $^3J_{HH}$ = 6.1 Hz), 7.93–7.68 (m, 12H, Ar), 7.65–7.36 (m, 9H, Ar). $^{31}P\{^1H\}$ NMR (162 MHz, $CDCl_3$): δ 38.1 (s).

Synthesis of 1,3-{$Ph_2P(Se)C(O)$}$_2(C_6H_4)$ (4)

Compound **4** was synthesized by a procedure similar to that of **3** using selenium (0.033 g, 0.417 mmol) and **1** (0.1 g, 0.198 mmol). Yield: 67% (0.087 g). Mp: 196–197 °C (dec). Anal. Calcd for $C_{32}H_{24}O_2P_2Se_2$: C, 58.20; H, 3.66. Found: C, 58.16; H, 3.68. FT IR (KBr disc) cm^{-1}: ν_{CO}: 1653 s. ^1H NMR (400 MHz, $CDCl_3$): δ 8.89 (s, 1H, Ar), 8.39 (d, 2H, Ar, $^3J_{HH}$ = 6.1 Hz), 7.85–7.76 (m, 12H, Ar), 7.58–7.46 (m, 9H, Ar). $^{31}P\{^1H\}$ NMR (162 MHz, $CDCl_3$): δ 31.1 (s), $^1J_{PSe}$ = 746 Hz.

Synthesis of [$Ru_2(\eta^6$-*p*-cymene$)_2Cl_4$\{1,3-{$Ph_2PC(O)$}$_2(C_6H_4)$}] (5)

A solution of **1** (0.040 g, 0.079 mmol) in CH_2Cl_2 (3 mL) was added dropwise to the solution of [$Ru(\eta^6$-*p*-cymene$)Cl_2]_2$ (0.024 g, 0.039 mmol) also in CH_2Cl_2 (4 mL) during which time the color of the solution turned from orange to brown. The reaction was allowed to stir for 3 h after which the

solution was concentrated to 5 mL and saturated with 2 mL of petroleum ether to afford brown crystals of **5**. Yield: 91% (0.080 g). Mp: 219–210 °C. Anal. Calcd for $C_{52}H_{52}Ru_2Cl_4O_2P_2$: C, 56.02; H, 4.70. Found: C, 56.12; H, 4.53. FT IR (KBr disc) cm^{-1}: ν_{CO}: 1699 s. ^1H NMR (400 MHz, $CDCl_3$): δ 8.24 (s, 1H, Ar), 7.84–7.79 (m, 8H, Ar), 7.71(d, 2H, Ar, $^3J_{HH}$ = 7.9 Hz), 7.31–7.25 (m, 12H, Ar), 6.88 (t, 1H, Ar, $^3J_{HH}$ = 7.9 Hz), 5.36 (d, 4H, Cym, $^3J_{HH}$ = 5.8 Hz), 5.26 (d, 4H, Cym, $^3J_{HH}$ = 5.8 Hz), 2.60 (m, 2H, CH), 1.69 (s, 6H, CH_3), 0.97 (d, 12H, CH_3, $^3J_{HH}$ = 7.0 Hz). $^{31}P\{^1H\}$ NMR (162 MHz, $CDCl_3$): δ 30.7.

Synthesis of $[Pd_2(\eta^3\text{-}C_3H_5)_2Cl_2\{1,3\text{-}\{Ph_2PC(O)\}_2(C_6H_4)\}]$ (6)

To a solution of $[Pd(\eta^3\text{-}C_3H_5)Cl]_2$ (0.018 g, 0.049 mmol) in CH_2Cl_2 (3 mL) was added a solution of **1** (0.050 g, 0.099 mmol) in the same solvent (4 mL) and the mixture was stirred for 2 h. The yellow colored solution obtained was concentrated to 3 mL and saturated with 1 mL of petroleum ether to yield **6** as a microcrystalline solid. Yield: 89% (0.078 g). Mp: 176–178 °C (dec). Anal. Calcd for $C_{38}H_{32}Pd_2Cl_2O_2P_2$: C, 52.68; H, 3.72. Found: C, 52.52; H, 3.61. FT IR (KBr disc) cm^{-1}: ν_{CO}: 1657 s. ^1H NMR (400 MHz, $CDCl_3$): δ 8.66 (s, 1H, Ar), 8.14 (d, 2H, Ar, $^3J_{HH}$ = 8.0 Hz), 7.69–7.64 (m, 8H, Ar), 7.48–7.38 (m, Ar, 12H), 7.27 (t, 1H, Ar, $^3J_{HH}$ = 8.0 Hz), 5.58–5.43 (m, 2H, allyl), 4.19 (br, s, 4H, allyl), 3.05 (br, s, 4H, allyl). $^{31}P\{^1H\}$ NMR (162 MHz, $CDCl_3$): δ 28.7.

Synthesis of $[PdCl\{2,6\text{-}\{Ph_2PC(O)\}_2(C_6H_3)\}]$ (7)

A solution of **1** (0.050 g, 0.099 mmol) in 5 mL of CH_2Cl_2 was added dropwise to a suspension of $AgClO_4$ (0.021 g, 0.099 mmol) in CH_2Cl_2 (4 mL) and the reaction mixture was allowed to stir for 30 minutes to give a light yellow solution. To this solution was added the solution of $[Pd(COD)Cl_2]$ (0.028 g, 0.099 mmol) in 4 mL of CH_2Cl_2. The reaction mixture was stirred for 6 h and the silver chloride was removed by filtration to give a clear yellow solution. The solution was concentrated to 3 mL and saturated with 5 mL of petroleum ether to get analytically pure **7** as a yellow solid. Yield: 62.5% (0.040 g). Mp: 238–239 °C (dec). Anal. Calcd for $C_{32}H_{23}ClO_2P_2Pd{\cdot}CH_2Cl_2$: C, 54.42; H, 3.46. Found: C, 54.66; H, 3.48. FT IR (KBr disc) cm^{-1}: ν_{CO}, 1659 s. ^1H NMR (400 MHz, $CDCl_3$): δ 8.12–7.98 (m, 6H, Ar), 7.86–7.80 (m, 4H, Ar), 7.57–7.31(m, 12H, Ar), 7.01 (m, 1H, Ar). $^{31}P\{^1H\}$ NMR (162 MHz, $CDCl_3$): δ 49.3(s).

Synthesis of $[NiBr\{2,6\text{-}\{Ph_2PC(O)\}_2(C_6H_3)\}]$ (8)

The bis(phosphomide) **2** (0.06 g, 0.103 mmol) and $[Ni(COD)_2]$ (0.028 g, 0.103 mmol) were placed in a round bottom flask and THF (7 mL) was added. The resulting solution was allowed to stir for 4 h during which the solution turned deep brown in color. The solvent was removed under reduced pressure and the brown residue obtained was washed with petroleum ether dissolved in CH_2Cl_2 (6 mL) and saturated with 3 mL of petroleum ether to produce orange crystals of **8**. Yield: 96% (0.064 g). Mp: 214–115 °C. Anal. Calcd for $C_{32}H_{23}BrNiO_2P_2$: C, 60.05; H, 3.62. Found: C, 59.98; H, 3.60. FT IR (KBr disc) cm^{-1}: ν_{CO}: 1686 s. ^1H NMR (400 MHz, $CDCl_3$): δ 7.97–7.92 (m, 8H, Ar), 7.86 (d, 2H, Ar, $^3J_{HH}$ = 7.4 Hz), 7.54–7.43 (m, 12H, Ar), 7.38 (m, 1H, Ar). $^{31}P\{^1H\}$ NMR (162 MHz, $CDCl_3$): δ 49.6 (s).

Synthesis of $[PdBr\{2,6\text{-}\{Ph_2PC(O)\}_2(C_6H_3)\}]$ (9)

Compound **9** was synthesized by a procedure similar to that of **8** using $[Pd_2(dba)_3]$ (0.053 g, 0.051 mmol) and **2** (0.060 g, 0.103 mmol). Yield: 95% (0.068 g). Mp: 253–254 °C (dec). Anal. Calcd for $C_{32}H_{23}BrPdO_2P_2$: C, 55.88; H, 3.37. Found: C, 55.51; H, 3.48. FT IR (KBr disc) cm^{-1}: ν_{CO}: 1653 s. ^1H NMR (400 MHz, $CDCl_3$): δ 8.02–7.97 (m, 10H, Ar), 7.54–7.41 (m, 13H, Ar). $^{31}P\{^1H\}$ NMR (162 MHz, $CDCl_3$): δ 52.2 (s).

Synthesis of $[Cu_2(\mu\text{-}Cl)_2\{1,3\text{-}\{Ph_2PC(O)\}_2(C_6H_4)\}_2]$ (10)

A solution of **1** (0.06 g, 0.119 mmol) in dichloromethane (6 mL) was added dropwise to a solution of CuCl (0.011 g, 0.119 mmol) in CH_3CN (4 mL). The reaction mixture was stirred for 3 h to give an orange-yellow solution. The solution was concentrated to 4 mL and stored at −20 °C to yield orange-yellow crystals of **10**. Yield: 80% (0.065 g). Mp: 228–230 °C (dec). Anal. Calcd for $C_{72}H_{60}Cl_2Cu_2N_4O_4P_4$: C, 63.25; H, 4.42. Found: C, 63.43; H, 3.31. FT IR (KBr disc) cm^{-1}: ν_{CO}: 1662 s. ^1H NMR (400 MHz, $CDCl_3$): δ 10.13 (s, 1H, Ar), 7.27 (d, 2H, Ar, $^3J_{HH}$ = 7.6 Hz), 7.26–7.16 (m, 12H, Ar), 7.10–7.07 (m, 9H, Ar). $^{31}P\{^1H\}$ NMR (162 MHz, $CDCl_3$): δ 4.0 (s).

Synthesis of $[Cu_2(\mu\text{-}Br)_2\{1,3\text{-}(Ph_2PC(O))_2(C_6H_4)\}_2]$ (11)

Compound **11** was synthesized by a procedure similar to that of **10** using CuBr (0.011 g, 0.079 mmol) and **1** (0.040 g, 0.079 mmol). Yield: 82% (0.041 g). Mp: 269–270 °C. Anal. Calcd for $C_{64}H_{48}Br_2Cu_2O_4P_4$: C, 59.50; H, 3.75. Found: C, 59.44; H, 3.86. FT IR (KBr disc) cm^{-1}: ν_{CO}: 1660 s. ^1H NMR (400 MHz, $CDCl_3$): δ 10.22 (s, 1H, Ar), 7.24 (d, 2H, Ar, $^3J_{HH}$ = 8.0 Hz), 7.20–7.16 (m, 12H, Ar), 7.09–7.05 (m, 9H, Ar). $^{31}P\{^1H\}$ NMR (162 MHz, $CDCl_3$): δ 1.9 (s).

Synthesis of $[Cu_2(\mu\text{-}I)_2\{1,3\text{-}(Ph_2PC(O))_2(C_6H_4)\}_2]$ (12)

Compound **12** was synthesized by a procedure similar to that of **10** using CuI (0.015 g, 0.079 mmol) and **1** (0.040 g, 0.079 mmol). Yield: 86% (0.047 g). Mp: 240–241 °C (dec). Anal. Calcd for $C_{64}H_{48}I_2Cu_2O_4P_4$: C, 55.47; H, 3.49. Found: C, 54.68; H, 3.24. FT IR (KBr disc) cm^{-1}: ν_{CO}: 1654 s. ^1H NMR (400 MHz, $CDCl_3$): δ 10.28 (s, 1H, Ar), 7.25 (d, 2H, Ar, $^3J_{HH}$ = 7.6 Hz), 7.21–7.14 (m, 12H, Ar), 7.10–7.06 (m, 9H, Ar). $^{31}P\{^1H\}$ NMR (162 MHz, $CDCl_3$): δ 1.3 (s).

Synthesis of $[Cu(CH_3CN)_2\{1,3\text{-}(Ph_2PC(O))_2(C_6H_4)\}]BF_4$ (13)

To a solution of **1** (0.050 g, 0.099 mmol) in dichloromethane (5 mL) was added dropwise a solution of $[Cu(CH_3CN)_4]BF_4$ (0.031 g, 0.099 mmol) in the same solvent (5 mL) and the reaction mixture was stirred for 3 h. The yellow solution obtained was concentrated under reduced pressure to a small bulk and kept at −20 °C to give **13** as a yellow crystalline solid. Yield: 74% (0.053 g). Mp: 219–220 °C (dec). Anal. Calcd for $C_{36}H_{30}BCuF_4N_2O_2P_2$: C, 58.83; H, 4.11; N, 3.81. Found: C, 58.26; H, 4.14; N, 3.62. FT IR (KBr disc) cm^{-1}: ν_{CO}: 1658 s. ^1H NMR (400 MHz, $CDCl_3$): δ 7.91 (s, br, 1H, Ar), 7.57 (s, br, 2H,

Ar), 7.47–7.43 (m, 4H, Ar), 7.39–7.27 (m, 16H, Ar), 7.00 (s, br, 1H, Ar). $^{31}P\{^{1}H\}$ NMR (162 MHz, $CDCl_3$): δ 10.5 (s).

Synthesis of $[Ag_2(\mu\text{-}ClO_4)_2\{1,3\text{-}(Ph_2PC(O))_2(C_6H_4)\}_2]$ (14)

A solution of **1** (0.040 g, 0.079 mmol) in 5 mL of THF was added dropwise to a solution of $AgClO_4$ (0.016 g, 0.079 mmol) in THF (5 mL) and the reaction mixture was allowed to stir for 1 h to give a light yellow solution. The solution was dried under reduced pressure and the residue redissolved in CH_2Cl_2 (4 mL) followed by saturation with 1 mL of petroleum ether to give light yellow crystals of $[Ag_2(\mu\text{-}Cl)(\mu\text{-}ClO_4)\{1,3\text{-}(Ph_2PC(O))_2(C_6H_4)\}_2]$ (**14a**) in very low yield (~4%) confirmed by single crystal X-ray study. This is due to the trace amount of AgCl contaminated with commercially obtained silver perchlorate. The bulk of the product was as expected $[Ag_2(\mu\text{-}ClO_4)_2\{1,3\text{-}(Ph_2PC(O))_2(C_6H_4)\}_2]$ (**14**) which did not give crystals suitable for single crystal X-ray diffraction studies. Yield: 88% (0.051 g). Mp: 175–177 °C (dec). Anal. Calcd for (**14**) $C_{64}H_{48}Ag_2Cl_2O_{12}P_4\cdot CH_2Cl_2$: C, 52.00; H, 3.36. Found: C, 51.93; H, 3.42. FT IR (KBr disc) cm^{-1}: ν_{CO}: 1660 s. ^1H NMR (400 MHz, $CDCl_3$): δ 8.07 (s, 1H, Ar), 7.94 (d, 2H, Ar, $^3J_{HH}$ = 7.9 Hz), 6.96 (t, 1H, Ar, $^3J_{HH}$ = 7.8 Hz), 7.72–7.39 (m, 20H, Ar). $^{31}P\{^{1}H\}$ NMR (162 MHz, $CDCl_3$): δ 15.8 (2 br s, 2P).

Crystals of **14a** were separated manually. Anal. Calcd for (**14a**) $C_{64}H_{48}Ag_2Cl_2O_8P_4\cdot 1.5CH_2Cl_2$: C, 53.04; H, 3.46. Found: C, 53.13; H, 3.46. Since the product was obtained in a very minute quantity, further spectroscopic studies could not be carried out.

Synthesis of $[Ag_2(\mu\text{-}CF_3SO_3)_2\{1,3\text{-}(Ph_2PC(O))_2(C_6H_4)\}_2]$ (15)

Compound **15** was synthesized by a procedure similar to that of **14** using AgOTf (0.015 g, 0.059 mmol) and **1** (0.030 g, 0.059 mmol). Yield: 83% (0.037 g). Mp: 179–180 °C (dec). Anal. Calcd for $C_{66}H_{48}Ag_2O_{10}P_4F_6S_2$: C, 52.19; H, 3.19; S, 4.22. Found: C, 51.85; H, 3.13; S, 4.06. FT IR (KBr disc) cm^{-1}: ν_{CO}: 1660 s. ^1H NMR (400 MHz, $CDCl_3$): δ 8.20 (s, 1H, Ar), 8.07 (d, 2H, Ar, $^3J_{HH}$ = 7.6 Hz), 7.60–7.49 (m, 20H, Ar), 6.31(t, 1H, Ar, $^3J_{HH}$ = 7.6 Hz). $^{31}P\{^{1}H\}$ NMR (162 MHz, $CDCl_3$): δ 14.8 (2 br s, 2P).

Synthesis of $[Ag_2(ClO_4)_2\{1,3\text{-}(Ph_2PC(O))_2(C_6H_4)\}]$ (16)

To a solution of $AgClO_4$ (0.032 g, 0.158 mmol) in THF (5 mL) was added a THF (4 mL) solution of **1** (0.040 g, 0.079 mmol) and the reaction mixture was stirred for 1 h to give a colorless solution. The solution was dried under reduced pressure and the solid dissolved in CH_2Cl_2 (5 mL) followed by addition of 1 mL of petroleum ether to give an analytically pure product of **16** as a colorless solid. Yield: 76% (0.060 g). Mp: 140–142 °C (dec). Anal. Calcd for $C_{32}H_{24}Ag_2Cl_2O_{10}P_2\cdot CH_2Cl_2$: C, 39.55; H, 2.62. Found: C, 39.64; H, 2.75. FT IR (KBr disc) cm^{-1}: ν_{CO}: 1662 s. ^1H NMR (400 MHz, $CDCl_3$): δ 8.25 (s, 1H, Ar), 8.11 (d, 2H, Ar, $^3J_{HH}$ = 7.8 Hz), 6.65–7.49 (m, 20H, Ar), 7.44 (t, 1H, Ar, $^3J_{HH}$ = 7.8 Hz). $^{31}P\{^{1}H\}$ NMR (162 MHz, $CDCl_3$): δ 19.7 (br s).

Synthesis of $[Ag_2(CF_3SO_3)_2\{1,3\text{-}(Ph_2PC(O))_2(C_6H_4)\}]$ (17)

Compound **17** was synthesized by a procedure similar to that of **16** using AgOTf (0.030 g, 0.119 mmol) and **1** (0.030 g, 0.059 mmol). The THF solution was concentrated to a small bulk (3 mL) and stored at −20 °C to give **17** as a colorless solid. Yield: 81% (0.050 g). Mp: 131–132 °C (dec). Anal. Calcd for $C_{34}H_{24}Ag_2F_6O_8P_2S_2\cdot 0.5C_4H_8O$: C, 41.09; H, 2.68; S, 6.09. Found: C, 41.23; H, 2.57; S, 6.79. FT IR (KBr disc) cm^{-1}: ν_{CO}: 1661 s. ^1H NMR (400 MHz, $CDCl_3$): δ 8.41 (s, 1H, Ar), 8.02 (d, 2H, Ar, $^3J_{HH}$ = 7.8 Hz), 7.49–7.37(m, 21H, Ar). $^{31}P\{^{1}H\}$ NMR (162 MHz, $CDCl_3$(−40 °C)): δ 18.8 (2d, 2P, $^1J(^{109}AgP)$ 730.5 Hz, $^1J(^{107}AgP)$ 641.4 Hz).

Synthesis of $[AuCl\{1,3\text{-}(Ph_2PC(O))_2(C_6H_4)\}]$ (18)

A solution of **1** (0.030 g, 0.059 mmol) in 4 mL of CH_2Cl_2 was added dropwise to a solution of $[AuCl(SMe_2)]$ (0.017 g, 0.059 mmol) also in CH_2Cl_2 (3 mL) and the reaction mixture was stirred for 2 h to give a light yellow solution. The solution was concentrated to a small bulk (3 mL) and saturated with 1 mL of petroleum ether to produce analytically pure **18** as a light yellow solid. Yield: 93% (0.040 g). Mp: 187–188 °C. Anal. Calcd for $C_{32}H_{24}AuClO_2P_2\cdot 0.25CH_2Cl_2$: C, 51.23; H, 3.27. Found: C, 51.45; H, 3.26. FT IR (KBr disc) cm^{-1}: ν_{CO}: 1656 s. ^1H NMR (400 MHz, $CDCl_3$): δ 8.66 (s, 1H, Ar), 8.17 (d, 2H, Ar, $^3J_{HH}$ = 7.9 Hz), 7.52–7.36 (m, 21H, Ar). $^{31}P\{^{1}H\}$ NMR (162 MHz, $CDCl_3$): δ 22.2.

Synthesis of $[Au_2Cl_2\{1,3\text{-}(Ph_2PC(O))_2(C_6H_4)\}]$ (19)

To a CH_2Cl_2 (4 mL) solution of **1** (0.030 g, 0.059 mmol) was added dropwise a solution of $[AuCl(SMe_2)]$ (0.035 g, 0.119 mmol) also in CH_2Cl_2 (5 mL) and the reaction mixture was stirred for 2 h to give a colorless solution. The solution was concentrated to 5 mL and saturated with 1 mL of petroleum ether to form **19** as a colorless solid. Yield: 89% (0.050 g). Mp: 149–150 °C. Anal. Calcd for $C_{32}H_{24}Au_2Cl_2O_2P_2$: C, 39.73; H, 2.50. Found: C, 40.06; H, 2.61. FT IR (KBr disc) cm^{-1}: ν_{CO}: 1656 s. ^1H NMR (400 MHz, $CDCl_3$): δ 8.77 (s, 1H, Ar), 8.35 (d, 2H, Ar, $^3J_{HH}$ = 7.9 Hz), 7.67–7.45 (m, 21H, Ar). $^{31}P\{^{1}H\}$ NMR (162 MHz, $CDCl_3$): δ 31.4.

Procedure for catalytic hydroformylation reactions

In a typical hydroformylation reaction, a high pressure reactor of 100 mL capacity was charged with ligand **1** (5 μmol, 2.5 mg), $[Rh(acac)(CO)_2]$ (2.5 μmol, 0.5 mL of a 5 mM solution in toluene) and olefin (5 mmol) in 20 mL of toluene, followed by decane (0.1 mL) as an internal standard. The reactor was flushed with synthesis gas (1 : 1 mixture of H_2 and CO gas) followed by charging to desired pressure at room temperature. The reactor was heated to desired temperature at a stirring speed of 350 rpm. After completion of the reaction, the reactor was cooled to room temperature in an ice-water bath and the remaining synthesis gas was carefully released in a well ventilated fume hood. The reaction mixture was quantitatively analyzed by gas chromatography.

Computational methods

All geometries were optimized using the Gaussian 09[39] suite of quantum chemical programs. All the geometries were optimized at the B3LYP[40] functional and characterized as true minima on the potential energy surfaces by evaluating the Hessian indices (the number of imaginary frequencies = 0). The 6-31G** basis set was used for all the atoms except the metal ion and iodine. The effective core potential basis set (SDD) is employed for iodine and metals (Pd, Ni, Ag, Ru and Cu).[41] Molecular orbital compositions of metals and ligands were analyzed using the AOMix-CDA program[42] using the wave functions generated at the B3LYP/6-31G**, SDD level of theory and using the Gaussian 03 suite of quantum chemical programs.[43]

X-ray crystallography

Crystals of each of the compounds **5**, **7–10**, **12**, and **14a** suitable for X-ray crystal analysis were mounted on a Cryoloop with a drop of paratone oil and placed in the cold nitrogen stream of the Kryoflex attachment of the Bruker APEX CCD diffractometer. A full sphere of data was collected using 606 scans in ω (0.3° per scan) at φ = 0, 120 and 240° (**10**, **14a**) or 363 scans in ω (0.5° per scan) at φ = 0, 120 and 240° (**7**) or a combination of three sets of 400 scans in ω (0.5° per scan) at φ = 0, 90, and 180° plus two sets of 800 scans in φ (0.45° per scan) at ω = −30 and 210° (**7–10**) using the APEX2[44] program suite. Crystals of **5** and **10** were found to be twins (CELL_NOW[45]). The raw data were reduced to F^2 values using SAINT+ software,[46] and a global refinement of unit cell parameters using *ca.* 2554–9996 reflections chosen from the full data set was performed. Multiple measurements of equivalent reflections provided the basis for an empirical absorption correction as well as a correction for any crystal deterioration during the data collection (SADABS[47] for **8**, **9**, **12** and **14a**; TWINABS[47] for **5** and **10**). The structure of **10** was solved by the Patterson method and the remaining structures were solved by direct methods and all were refined by full-matrix least-squares procedures using the SHELXTL program package.[48] Crystal data and refine parameters are shown in Table 4. Crystallographic data (excluding structure factors) for the structures reported in this paper have been deposited with the Cambridge Crystallographic Data Centre as supplementary publication no. CCDC 934905–934911.

Acknowledgements

We are grateful to the Department of Science and Technology (DST), New Delhi, for financial support of this work through grant no. SR/S1/IC-17/2010. P.K. thanks CSIR, New Delhi for research fellowships (JRF & SRF). We also thank the Department of Chemistry Instrumentation Facilities, IIT Bombay, for spectral and analytical data and J.T.M. thanks the Louisiana Board of Regents for the purchase of the CCD diffractometer and the Chemistry Department of Tulane University for support of the X-ray laboratory.

References

1 (*a*) G. R. Newkome, W. E. Puckett, V. K. Gupta and G. E. Kiefer, *Chem. Rev.*, 1986, **86**, 451–489; (*b*) M. Bertoli, A. Choualeb, D. G. Gusev, A. J. Lough, Q. Major and B. Moore, *Dalton Trans.*, 2011, **40**, 8941–8949.

2 (*a*) M. Albrecht and G. van Koten, *Angew. Chem., Int. Ed.*, 2001, **40**, 3750–3781; (*b*) M. Albrecht, R. A. Gossage, M. Lutz, A. L. Spek and G. van Koten, *Chem.–Eur. J.*, 2000, **6**, 1431–1445; (*c*) P. Steenwinkel, D. M. Grove, M. Veldman, A. L. Spek and G. van Koten, *Organometallics*, 1998, **17**, 5647–5655.

3 (*a*) N. Selander and K. J. Szabo, *Chem. Rev.*, 2011, **111**, 2048–2076; (*b*) W. Leis, H. A. Mayer and W. C. Kaska, *Coord. Chem. Rev.*, 2008, **252**, 1787–1797; (*c*) B. J. Boro, E. N. Duesler, K. I. Goldberg and R. A. Kemp, *Inorg. Chem.*, 2009, **48**, 5081–5087; (*d*) J. M. Longmire, X. Zhang and M. Shang, *Organometallics*, 1998, **17**, 4374–4379; (*e*) E. Poverenov, G. Leitus, L. J. W. Shimon and D. Milstein, *Organometallics*, 2005, **24**, 5937–5944; (*f*) P. Bhattacharya, J. A. Krause and H. Guan, *Organometallics*, 2011, **30**, 4720–4729; (*g*) R. A. Baber, R. B. Bedford, M. Betham, M. E. Blake, S. J. Coles, M. F. Haddow, M. B. Hursthouse, A. G. Orpen, L. T. Pilarski, P. G. Pringle and R. L. Wingad, *Chem. Commun.*, 2006, 3880–3882.

4 (*a*) D. Benito-Garagorri and K. Kirchner, *Acc. Chem. Res.*, 2008, **41**, 201–213; (*b*) E. Kinoshita, K. Arashiba, S. Kuriyama, Y. Miyake, R. Shimazaki, H. Nakanishi and Y. Nishibayashi, *Organometallics*, 2012, **31**, 8437–8443; (*c*) K. Arashiba, K. Sasaki, S. Kuriyama, Y. Miyake, H. Nakanishi and Y. Nishibayashi, *Organometallics*, 2012, **31**, 2035–2041; (*d*) P. Kang, C. Cheng, Z. Chen, C. K. Schauer, T. J. Meyer and M. Brookhart, *J. Am. Chem. Soc.*, 2012, **134**, 5500–5503; (*e*) M. Findlater, W. H. Bernskoetter and M. Brookhart, *J. Am. Chem. Soc.*, 2010, **132**, 4534–4535; (*f*) D. Benito-Garagorri, J. Wiedermann, M. Pollak, K. Mereiter and K. Kirchner, *Organometallics*, 2006, **26**, 217–222; (*g*) D. Benito-Garagorri, K. Mereiter and K. Kirchner, *Eur. J. Inorg. Chem.*, 2006, 4374–4379.

5 (*a*) J. Alos, T. Bolano, M. A. Esteruelas, M. Olivan, E. Oñate and M. Valencia, *Inorg. Chem.*, 2013, **52**, 6199–6213; (*b*) A. E. W. Ledger, A. Moreno, C. E. Ellul, M. F. Mahon, P. S. Pregosin, M. K. Whittlesey and J. M. J. Williams, *Inorg. Chem.*, 2010, **49**, 7244–7256; (*c*) R. Venkateswaran, J. T. Mague and M. S. Balakrishna, *Inorg. Chem.*, 2007, **46**, 809–817; (*d*) Q. Major, A. J. Lough and D. G. Gusev, *Organometallics*, 2005, **24**, 2492–2501; (*e*) K. Arashiba, K. Sasaki, S. Kuriyama, Y. Miyake, H. Nakanishi and Y. Nishibayashi, *Organometallics*, 2012, **31**, 2035–2041; (*f*) R. Dallanegra, A. B. Chaplin and A. S. Weller, *Organometallics*, 2012, **31**, 2720–2728; (*g*) Q. Major, A. J. Lough and D. G. Gusev, *Organometallics*, 2005, **24**, 2492–2501.

6 (*a*) R. Ahuja, B. Punji, M. Findlater, C. Supplee, W. Schinski, M. Brookhart and A. S. Goldman, *Nat. Chem.*, 2011, **3**, 167–171; (*b*) D. Morales-Morales, *Rev. Soc. Quím.*

Méx., 2004, **48**, 338–346; (*c*) O. V. Ozerov, C. Guo and B. M. Foxman, *J. Organomet. Chem.*, 2006, **691**, 4802–4806; (*d*) D. M. Spasyuk and D. Zargarian, *Inorg. Chem.*, 2010, **49**, 6203–6213.

7 (*a*) J. Aydin, K. S. Kumar, L. Eriksson and K. J. Szabó, *Adv. Synth. Catal.*, 2007, **349**, 2585–2594; (*b*) J. Aydin, A. Ryden and K. J. Szabo, *Tetrahedron: Asymmetry*, 2008, **19**, 1867–1870; (*c*) J.-J. Feng, X.-F. Chen, M. Shi and W.-L. Duan, *J. Am. Chem. Soc.*, 2000, **132**, 5562–5563.

8 (*a*) R. B. Bedford, S. M. Draper, P. Noelle Scully and S. L. Welch, *New J. Chem.*, 2000, **24**, 745–747; (*b*) J. L. Bolliger, O. Blacque and C. M. Frech, *Angew. Chem., Int. Ed.*, 2007, **46**, 6514–6517; (*c*) D. Olsson and O. F. Wendt, *J. Organomet. Chem.*, 2009, **694**, 3112–3115; (*d*) E. M. Schuster, M. Botoshansky and M. Gandelman, *Angew. Chem., Int. Ed.*, 2008, **47**, 4555–4558; (*e*) D. Benito-Garagorri, J. Wiedermann, M. Pollak, K. Mereiter and K. Kirchner, *Organometallics*, 2006, **26**, 217–222; (*f*) J. L. Bolliger and C. M. Frech, *Adv. Synth. Catal.*, 2009, **351**, 891–902; (*g*) B.-S. Zhang, C. Wang, J.-F. Gong and M.-P. Song, *J. Organomet. Chem.*, 2009, **694**, 2555–2561.

9 I. P. Beletskaya and A. V. Cheprakov, *Chem. Rev.*, 2000, **100**, 3009–3066.

10 J. Choi, D. Y. Wang, S. Kundu, Y. Choliy, T. J. Emge, K. Krogh-Jespersen and A. S. Goldman, *Science*, 2011, **332**, 1545–1548.

11 (*a*) D. S. McGuiness, V. C. Gibson and J. W. Steed, *Organometallics*, 2004, **23**, 6288–6292; (*b*) D. S. McGuiness, V. C. Gibson, D. F. Wass and J. W. Steed, *J. Am. Chem. Soc.*, 2003, **125**, 12716–12717.

12 A. S. Goldman, A. H. Roy, Z. Huang, R. Ahuja, W. Schinski and M. Brookhart, *Science*, 2006, **312**, 257–261.

13 (*a*) F. Liu, E. B. Pak, B. Singh, C. M. Jensen and A. S. Goldman, *J. Am. Chem. Soc.*, 1999, **121**, 4086–4087; (*b*) C. Jensen, *Chem. Commun.*, 1999, 2443–2449; (*c*) J. Choi, A. H. R. MacArthur, M. Brookhart and A. S. Goldman, *Chem. Rev.*, 2011, **111**, 1761–1779.

14 R. Tanaka, M. Yamashsita and K. Nozaki, *J. Am. Chem. Soc.*, 2009, **131**, 14168–14169.

15 K. Arshiba, Y. Miyake and Y. Nishibayashi, *Nat. Chem.*, 2011, **3**, 120–125.

16 (*a*) D. Vuzman, E . Poverenov, L. J. W. Shimon, Y. D. Posner and D. Milstein, *Organometallics*, 2008, **27**, 2627–2634; (*b*) M. Feller, E. Ben-Ari, Y. Diskin-Posner, G. Leitus, L. J. W. Shimon, L. Konstantinovski and D. Mistein, *Inorg. Chem.*, 2010, **49**, 1615–16254; (*c*) C. Gunanathan and D. Milstein, *Acc. Chem. Res.*, 2011, **44**, 588–602; (*d*) D. Milstein, *Top Catal.*, 2010, **53**, 915–923.

17 C. Gunanathan, Y. Ben-David and D. Milstein, *Science*, 2007, **317**, 790–792.

18 E. Lindner and H. Lesiecki, *Chem. Ber.*, 1979, **112**, 773–775.

19 (*a*) H. Albers, W. Künzel and W. Schuler, *Chem. Ber.*, 1952, **85**, 239–249; (*b*) R. G. Kostyanovsky, V. V. Yakshin and S. L. Zimont, *Tetrahedron*, 1968, **24**, 2995–3000; (*c*) H. Kunzek, M. Braun, E. Nesener and K. Rühlmann, *J. Organomet. Chem.*, 1973, **49**, 149–156; (*d*) K. Issleib, H. Schmidt and H. Meyer, *J. Organomet. Chem.*, 1978, **160**, 47–57; (*e*) A. Varshney and G. M. Gray, *Inorg. Chim. Acta*, 1988, **148**, 215–222; (*f*) A. R. Barron, S. W. Hall and A. H. Cowley, *J. Chem. Soc., Chem. Commun.*, 1987, 1753–1754; (*g*) R. Angharad Baber, M. L. Clarke, A. Guy Orpen and D. A. Ratcliffe, *J. Organomet. Chem.*, 2003, **667**, 112–119; (*h*) A. C. Tsipis, *Organometallics*, 2006, **25**, 2774–2781.

20 (*a*) G. S. Ananthnag, S. Kuntavalli, J. T. Mague and M. S. Balakrishna, *Inorg. Chem.*, 2012, **51**, 5919–5930; (*b*) M. S. Balakrishna, P. Kumar, B. Punji and J. T. Mague, *J. Organomet. Chem.*, 2010, **695**, 981–986; (*c*) B. Punji, J. T. Mague and M. S. Balakrishna, *Inorg. Chem.*, 2006, **45**, 9454–9464; (*d*) S. Rao, C. Ganesamoorthy, S. M. Mobin and M. S. Balakrishna, *Dalton Trans.*, 2011, **40**, 5841–5843; (*e*) C. Ganesamoorthy, M. S. Balakrishna and J. T. Mague, *Inorg. Chem.*, 2009, **48**, 3768–3782; (*f*) B. Punji, J. T. Mague and M. S. Balakrishna, *Inorg. Chem.*, 2007, **46**, 11316–11327; (*g*) P. Chandrasekaran, J. T. Mague and M. S. Balakrishna, *Inorg. Chem.*, 2005, **44**, 7925–7932; (*h*) R. Venkateswaran, J. T. Mague and M. S. Balakrishna, *Inorg. Chem.*, 2007, **46**, 809–817.

21 (*a*) A. Bugarin and B. T. Connell, *Organometallics*, 2008, **27**, 4357–4369; (*b*) Y. Motoyama, M. Okano, H. Narusawa, N. Makihara, K. Aoki and H. Nishiyama, *Organometallics*, 2001, **20**, 1580–1591.

22 (*a*) M. S. Balakrishna, R. Panda and J. T. Mague, *J. Chem. Soc., Dalton Trans.*, 2002, 4617–4621; (*b*) M. S. Balakrishna, P. P. George and J. T. Mague, *J. Organomet. Chem.*, 2004, **689**, 3388–3394; (*c*) M. S. Balakrishna, P. P. George and S. M. Mobin, *Polyhedron*, 2005, **24**, 475–480; (*d*) M. S. Balakrishna, D. Suresh, P. Kumar and J. T. Mague, *J. Organomet. Chem.*, 2011, **696**, 3616–3622; (*e*) M. N. Chevykalova, L. F. Manzhukova, N. V. Artemova, Y. N. Luzikov, I. E. Nifant and E. E. Nifant, *Russ. Chem. Bull.*, 2003, **52**, 78–84.

23 R. A. Baber, R. B. Bedford, M. Betham, M. E. Blake, S. J. Coles, M. F. Haddow, M. B. Hursthouse, A. G. Orpen, L. T. Pilarski, P. G. Pringle and R. L. Wingad, *Chem. Commun.*, 2006, 3880–3882.

24 (*a*) M. Albrecht, *Chem. Rev.*, 2009, **110**, 576–623; (*b*) D. Balcells, E. Clot and O. Eisenstein, *Chem. Rev.*, 2009, **110**, 749–823.

25 (*a*) S. I. M. Paris, F. R. Lemke, R. Sommer, P. Lönnecke and E. Hey-Hawkins, *J. Organomet. Chem.*, 2005, **690**, 1807–1813; (*b*) T. J. Geldbach, A. B. Chaplin, K. D. Hänni, R. Scopelliti and P. J. Dyson, *Organometallics*, 2005, **24**, 4974–4980; (*c*) M. S. Balakrishna, D. Suresh, P. Kumar and J. T. Mague, *J. Organomet. Chem.*, 2011, **696**, 3616–3622; (*d*) E. E. Joslin, C. L. McMullin, T. B. Gunnoe, T. R. Cundari, M. Sabat and W. H. Myers, *Inorg. Chem.*, 2012, **51**, 4791–4801.

26 (*a*) F. Bachechi, *Struct. Chem.*, 2003, **14**, 263–269; (*b*) A. R. Kennedy, R. J. Cross and K. W. Muir, *Inorg. Chim. Acta*, 1995, **231**, 195–200; (*c*) A. B. Salah and D. Zargarian, *Dalton Trans.*, 2011, **40**, 8977–8985; (*d*) V. Gómez-Benítez, O. Baldovino-Pantaleón, C. Herrera-Álvarez, R. A. Toscano

and D. Morales-Morales, *Tetrahedron Lett.*, 2006, **47**, 5059–5062; (*e*) A. Salah and D. Zargarian, *Acta Crystallogr., Sect. E: Struct. Rep. Online*, 2011, **67**, m437; (*f*) A. G. Orpen, L. Brammer, F. H. Allen, O. Kennard, D. G. Watson and R. Taylor, *J. Chem. Soc., Dalton Trans.*, 1989, S1–S83.

27 (*a*) M. T. Johnson, Z. Džolić, M. Cetina, O. F. Wendt, L. Öhrström and K. Rissanen, *Cryst. Growth Des.*, 2012, **12**, 362–368; (*b*) F. Gorla, L. M. Venanzi and A. Albinati, *Organometallics*, 1994, **13**, 43–54; (*c*) R. J. Cross, A. R. Kennedy and K. W. Muir, *J. Organomet. Chem.*, 1995, **487**, 227–233.

28 F. Caruso, M. Camalli, H. Rimml and L. M. Venanzi, *Inorg. Chem.*, 1995, **34**, 673–679.

29 (*a*) M. Rubio, A. Suarez, E. Alvarez, C. Bianchini, W. Oberhauser, M. Peruzzini and A. Pizzano, *Organometallics*, 2007, **26**, 6428–6436; (*b*) T. Robert, Z. Abiri, J. Wassenaar, A. J. Sandee, S. Romanski, J.-M. Neudörfl, H.-G. Schmalz and J. N. H. Reek, *Organometallics*, 2009, **28**, 478–483; (*c*) A. G. Panda, M. D. Bhor, S. S. Ekbote and B. M. Bhanage, *Catal Lett.*, 2009, **131**, 649–655.

30 S. Yu, Y.-m. Chie, Z.-h. Guan, Y. Zou, W. Li and X. Zhang, *Org. Lett.*, 2008, **11**, 241–244.

31 The optimized geometries are provided in Fig. S1 in the ESI.†

32 W. L. Almarego and D. D. Perin, *Purification of Laboratory Chemicals*, 4th edn, Butterworth-Heinemann Linacre House, Jordan Hill, Oxford, U.K., 1996.

33 B. S. Furniss, A. J. Hannaford, P. W. G. Smith and A. R. Tatchell, *Vogel's Textbook of Practical Organic Chemistry*, 5th edn, ELBS, England, 1989, p. 428–429.

34 G. J. Kubas, B. Monzyk and A. L. Crumblis, *Inorg. Synth.*, 1990, **28**, 68–70.

35 M.-C. Brandys, M. C. Jennings and R. J. Puddephatt, *J. Chem. Soc., Dalton Trans.*, 2000, 4601–4606.

36 M. A. Bennett, T. N. Huang, T. W. Matheson, A. K. Smith, S. Ittel and W. Nickerson, *Inorg. Synth.*, 1982, **21**, 74–78.

37 Y. Tatsuno, T. Yoshida, S. Otsuka, N. Al-Salem and B. L. Shaw, *Inorg. Synth.*, 1990, **28**, 342–345.

38 S. Komiya, *Synthesis of Organometallic Compounds*, Wiley, Chichester, U.K., 1997.

39 M. J. Frisch, G. W. Trucks, H. B. Schlegel, G. E. Scuseria, M. A. Robb, J. R. Cheeseman, G. Scalmani, V. Barone, B. Mennucci, G. A. Petersson, H. Nakatsuji, M. Caricato, X. Li, H. P. Hratchian, A. F. Izmaylov, J. Bloino, G. Zheng, J. L. Sonnenberg, M. Hada, M. Ehara, K. Toyota, R. Fukuda, J. Hasegawa, M. Ishida, T. Nakajima, Y. Honda, O. Kitao, H. Nakai, T. Vreven, J. A. Montgomery Jr., J. E. Peralta, F. Ogliaro, M. Bearpark, J. J. Heyd, E. Brothers, K. N. Kudin, V. N. Staroverov, R. Kobayashi, J. Normand, K. Raghavachari, A. Rendell, J. C. Burant, S. S. Iyengar, J. Tomasi, M. Cossi, N. Rega, J. M. Millam, M. Klene, J. E. Knox, J. B. Cross, V. Bakken, C. Adamo, J. Jaramillo, R. Gomperts, R. E. Stratmann, O. Yazyev, A. J. Austin, R. Cammi, C. Pomelli, J. W. Ochterski, R. L. Martin, K. Morokuma, V. G. Zakrzewski, G. A. Voth, P. Salvador, J. J. Dannenberg, S. Dapprich, A. D. Daniels, Ö. Farkas, J. B. Foresman, J. V. Ortiz, J. Cioslowski and D. J. Fox, *GAUSSIAN 09 (Revision A.02)*, Gaussian, Inc., Wallingford, CT, 2009.

40 (*a*) A. D. Becke, *Phys. Rev. A*, 1988, **38**, 3098; (*b*) A. D. Becke, *J. Chem. Phys.*, 1993, **98**, 5648; (*c*) C. Lee, W. Yang and R. G. Parr, *Phys. Rev. B: Condens. Matter*, 1988, **37**, 785–789.

41 (*a*) H. Stoll, P. Fuentealba, P. Schwerdtfeger, J. Flad, L. V. Szentpaly and H. J. Preuss, *Chem. Phys.*, 1984, **81**, 2732; (*b*) M. Dolg, U. Wedig, H. Stoll and H. J. Preuss, *Chem. Phys.*, 1987, **86**, 866; (*c*) D. Andrae, U. Haussermann, M. Dolg, H. Stoll and H. J. Preuss, *Theor. Chim. Acta*, 1990, **77**, 123.

42 (*a*) S. I. Gorelsky, *AOMix: Program for Molecular Orbital Analysis*, York University, Toronto, Canada, 1997, http://www.sq-chem.net; (*b*) S. I. Gorelsky and A. B. P. Lever, *J. Organomet. Chem.*, 2001, **635**, 187.

43 M. J. Frisch, G. W. Trucks, H. B. Schlegel, G. E. Scuseria, M. A. Robb, J. R. Cheeseman, J. A. Montgomery Jr., T. Vreven, K. N. Kudin, J. C. Burant, J. M. Millam, S. S. Iyengar, J. Tomasi, V. Barone, B. Mennucci, M. Cossi, G. Scalmani, N. Rega, G. A. Petersson, H. Nakatsuji, M. Hada, M. Ehara, K. Toyota, R. Fukuda, J. Hasegawa, M. Ishida, T. Nakajima, Y. Honda, O. Kitao, H. Nakai, M. Klene, X. Li, J. E. Knox, H. P. Hratchian, J. B. Cross, V. Bakken, C. Adamo, J. Jaramillo, R. Gomperts, R. E. Stratmann, O. Yazyev, A. J. Austin, R. Cammi, C. Pomelli, J. W. Ochterski, P. Y. Ayala, K. Morokuma, G. A. Voth, P. Salvador, J. J. Dannenberg, V. G. Zakrzewski, S. Dapprich, A. D. Daniels, M. C. Strain, O. Farkas, D. K. Malick, A. D. Rabuck, K. Raghavachari, J. B. Foresman, J. V. Ortiz, Q. Cui, A. G. Baboul, S. Clifford, J. Cioslowski, B. B. Stefanov, G. Liu, A. Liashenko, P. Piskorz, I. Komaromi, R. L. Martin, D. J. Fox, T. Keith, M. A. Al-Laham, C. Y. Peng, A. Nanayakkara, M. Challacombe, P. M. W. Gill, B. Johnson, W. Chen, M. W. Wong, C. Gonzalez and J. A. Pople, *GAUSSIAN 03 (Revision C.02)*, Gaussian, Inc., Wallingford CT, 2004.

44 *Bruker-AXS SMART, Version 5.625*, Madison, WI, 2000.

45 *APEX2 version 2.1–0*, Bruker-AXS, Madison, WI, 2006.

46 *Bruker-AXS, S., Version 7.03*, Madison, WI, 2006.

47 G. W. Sheldrick, *SADABS, versions 2.05 and 2007/2*, University of Göttingen, Germany, 2002.

48 *Bruker-AXS, S., Version 6.10*, Madison, WI, 2000.